# Magnetic response and quantum critical behavior in the doped two-leg extended Hubbard ladder

M. Tsuchiizu and Y. Suzumura
*Department of Physics, Nagoya University, Nagoya 464-8602, Japan*
(Received 1 June 2004; revised manuscript received 12 October 2004; published 16 August 2005)

We have investigated quantum critical behavior in the doped two-leg extended Hubbard ladder, by using a weak-coupling bosonization method. In the ground state, the dominant fluctuation changes from the conventional *d*-wave-like superconducting (SC*d*) state into density-wave states, with increasing nearest-neighbor repulsions and/or decreasing doping rate. The competition between the SC*d* state and the charge-density-wave state coexisting with the *p*-density-wave state becomes noticeable on the critical point, at which the gap for magnetic excitations vanishes. Based on the Majorana-fermion description of the effective theory, we calculate the temperature dependence of the magnetic response such as the spin susceptibility and the NMR relaxation rate, which exhibit unusual properties due to two kinds of spin excitation modes. On the quantum critical point, the spin susceptibility shows paramagnetic behavior with logarithmic corrections and the NMR relaxation rate also exhibits anomalous power-law behavior. We discuss the commensurability effect due to the umklapp scattering and relevance to the two-leg ladder compounds $Sr_{14-x}Ca_xCu_{24}O_{41}$.

DOI: 10.1103/PhysRevB.72.075121 PACS number(s): 71.10.Fd, 71.10.Hf, 71.10.Pm, 71.30.+h

## I. INTRODUCTION

The two-leg ladder compounds, $Sr_{14-x}Ca_xCu_{24}O_{41}$, which exhibit the superconducting state[1] under pressure for $x \gtrsim 12$, have been studied intensively since superconductivity was confirmed in a system with ladder structure.[2–6] This material, consisting of chain and ladder layers, already has holes which are doped on the ladder layer even for the parent material, $x=0$. Reflecting its ladder structure, there exists a large gap in the magnetic excitations.[7,8] It is known that Ca substitution yields an increase of the doping rate from $\delta \approx 0.07$ ($x=0$) to $\delta \approx 0.25$ ($x=12$),[9] and the material becomes favorable for the superconducting state. A recent NMR measurement on superconducting materials under high pressure reveals evidence for a large spin gap ($\approx 200$ K),[10–12] which is much higher than the superconducting transition temperature $T_c$. From the measurement of the $^{63}$Cu NMR relaxation rate $T_1^{-1}$ at ladder sites, Fujiwara *et al.*[12] suggested that there are two excitation modes in the normal state: The one at higher temperature is an activation-type mode due to the spin gap and the other at lower temperature is an anomalous paramagnetic mode. In addition to the superconducting state, intensive studies have been devoted to the charge-density-wave (CDW) state, which is found in the parent system ($x=0$) from optical measurements.[13–15] Further the global phase diagram for overall hole doping[16,17] shows that, with increasing the hole doping, the CDW state is suppressed and disappears at $x \simeq 9$, while the superconducting state emerges for $x \simeq 11$ and under pressure. From Raman scattering measurements,[18] it has been suggested that collective modes of the CDW state exist even in the highly doped superconducting material $x=12$. Thus, it is expected that, by varying $x$ and temperature, the competition between the superconducting (SC) state and the CDW state will become crucial in these compounds, and nontrivial critical behavior will emerge in the competing region.

Theoretical approaches to doped two-leg ladder systems have been performed by using various kinds of methods. It has been established that the *d*-wave-like superconducting (SC*d*) state becomes the most dominant fluctuation in the ground state of the doped two-leg Hubbard ladder and *t*-*J* ladder systems.[19–30] When the model is extended to include parameters of several intersite Coulomb repulsions, other fluctuations can overcome the SC*d* state. A global phase diagram obtained from a weak-coupling *g*-ology approach shows that the CDW state, *s*-wave-singlet state, and *d*-density-wave states can also become quasi-long-range-ordered states in parameter space.[28,30,31] The CDW state has been confirmed by studying numerically the Hubbard model with nearest-neighbor repulsions.[32] A richer phase diagram is obtained for the system at half filling[31,33] and at quarter filling.[34] Despite the huge number of theoretical works on the ordered state, the critical behavior expected close to the boundary between different phases is still unknown. In addition, the temperature dependence of magnetic quantities, such as the uniform spin susceptibility and the NMR relaxation rate, has been examined mainly on undoped spin ladder systems and the case with finite doping is not yet clarified.

In the present paper, we investigate electronic states both at zero temperature and at finite temperature for the two-leg extended Hubbard model with finite doping, where special attention is focused on states near the phase boundary between the SC*d* state and the density-wave state. Based on the Majorana-fermion description, which is used for the low-energy effective theory of the spin degrees of freedom, we demonstrate the unconventional temperature dependence of both the spin susceptibility and the NMR relaxation rate close to the quantum critical region and also on the critical point, including logarithmic corrections.

This paper is organized as follows. In Sec. II, we introduce a model Hamiltonian for doped ladder systems and derive an effective theory describing low-energy physics, using weak-coupling *g*-ology supplemented by bosonization and refermionization. In Sec. III, we investigate the ground-state phase diagram by using the renormalization-group (RG) method, and clarify that the system exhibits a quantum criti-

 

cal behavior on the boundary between the SC$d$ state and the coexisting state of CDW and $p$-density wave. In Sec. IV, the temperature dependence of both the spin susceptibility and the NMR relaxation rate is examined to clarify their anomalous behavior in the proximity to the quantum critical point. Finally in Sec. V, we give a summary and discuss the commensurability effect due to umklapp scattering and the relevance of the present calculation to the experimental results for $Sr_{14-x}Ca_xCu_{24}O_{41}$.

## II. MODEL HAMILTONIAN AND FORMULATION

We consider a model of a doped two-leg Hubbard ladder with on-site and intersite Coulomb repulsions. The Hamiltonian is given by

$$H = H_0 + H_{\text{int}}. \tag{2.1}$$

The first term $H_0$ describes electron hopping along and between the legs:

$$H_0 = -t_{\parallel}\sum_{j,\sigma,l}(c^{\dagger}_{j,l,\sigma}c_{j+1,l,\sigma} + \text{H.c.}) - t_{\perp}\sum_{j,\sigma}(c^{\dagger}_{j,1,\sigma}c_{j,2,\sigma} + \text{H.c.}), \tag{2.2}$$

where $c_{j,l,\sigma}$ annihilates an electron of spin $\sigma$ $(=\uparrow,\downarrow)$ on the $j$th rung and $l$th leg with $l=1$, 2. The Hamiltonian $H_{\text{int}}$ represents interactions between electrons:

$$H_{\text{int}} = U\sum_{j,l} n_{j,l,\uparrow}n_{j,l,\downarrow} + V_{\parallel}\sum_{j,l} n_{j,l}n_{j+1,l} + V_{\perp}\sum_{j} n_{j,1}n_{j,2}, \tag{2.3}$$

where $U$ $(>0)$, $V_{\parallel}$ $(\geqslant 0)$, and $V_{\perp}$ $(\geqslant 0)$ are coupling constants for the on-site repulsion, the nearest-neighbor repulsion on respective chains, and the nearest-neighbor repulsion on a rung, respectively. The density operators are $n_{j,l,\sigma} = c^{\dagger}_{j,l,\sigma}c_{j,l,\sigma}$, and $n_{j,l} = n_{j,l,\uparrow} + n_{j,l,\downarrow}$.

Considering the two-particle interactions $H_{\text{int}}$ as a weak perturbation, we first diagonalize the single-particle hopping part $H_0$. The diagonalization can be performed in terms of the the Fourier transform, $c_{\sigma}(\boldsymbol{k}) = (2N)^{-1/2}\Sigma_{j,l}e^{-ik_{\parallel}j - ik_{\perp}l}c_{j,l,\sigma}$ where $\boldsymbol{k} = (k_{\parallel}, k_{\perp})$ with $k_{\perp} = 0, \pi$, and the lattice spacing $a$ is set equal to 1. Then $H_0$ is rewritten as $H_0 = \Sigma_{\boldsymbol{k},\sigma}\varepsilon(\boldsymbol{k})c^{\dagger}_{\sigma}(\boldsymbol{k})c_{\sigma}(\boldsymbol{k})$, where

$$\varepsilon(\boldsymbol{k}) = -2t_{\parallel}\cos k_{\parallel} - t_{\perp}\cos k_{\perp}. \tag{2.4}$$

Here we consider the hole doping $\delta$ for $t_{\perp} < 2t_{\parallel}\cos^2(\pi\delta/2)$ where both the bonding $(k_{\perp}=0)$ and antibonding $(k_{\perp}=\pi)$ energy bands are partially filled. In this case, the Fermi points are located at $k_{\parallel} = \pm k_{F,0}$ and $\pm k_{F,\pi}$ for the bonding and antibonding bands, respectively, where

$$k_{F,0} = \frac{\pi}{2}(1-\delta) + \lambda, \quad k_{F,\pi} = \frac{\pi}{2}(1-\delta) - \lambda, \tag{2.5}$$

and the quantity $\lambda$ is given by

$$\lambda \equiv \sin^{-1}\left[ t_{\perp}/\left(2t_{\parallel}\cos\frac{\pi}{2}\delta\right)\right]. \tag{2.6}$$

The Fermi velocity of the bonding band and that of the antibonding band are given by $v_{F,0} = 2t_{\parallel}\cos(\pi\delta/2 - \lambda)$ and $v_{F,\pi} = 2t_{\parallel}\cos(\pi\delta/2 + \lambda)$, respectively. For $\delta = 0$, the Fermi velocity takes the common value $v_{F,0} = v_{F,\pi} = v_F$, where $v_F = 2t_{\parallel}[1 - (t_{\perp}/2t_{\parallel})^2]^{1/2}$ for arbitrary $t_{\perp}$ $(<2t_{\parallel})$. In the following, the difference between $v_{F,0}$ and $v_{F,\pi}$ is not taken into account since we restrict ourselves to the small-doping case $|\delta| \ll 1$.

Let us define order parameters of possible states. The most favorable state in doped ladders is the SC$d$ state whose order parameter is given by[33]

$$O_{\text{SC}d} = \sum_{j}(c_{j,1,\uparrow}c_{j,2,\downarrow} - c_{j,1,\downarrow}c_{j,2,\uparrow}). \tag{2.7}$$

Other possible ground states are density-wave states with different angular momenta.[31,33] In this paper we consider $s$-density-wave and $p$-density-wave (PDW) states. The $s$-density-wave state is nothing but the conventional CDW state. The order parameters of the density-wave states are given by

$$O_A = \sum_{\boldsymbol{k},\sigma,\pm} f_A(\boldsymbol{k})c^{\dagger}_{\sigma}(\boldsymbol{k})c_{\sigma}(\boldsymbol{k} \pm \boldsymbol{Q}), \tag{2.8}$$

where $A$ is the CDW or PDW, and $\boldsymbol{Q} = (2k_F, \pi)$ with $k_F = \frac{1}{2}\pi(1-\delta)$. The form factors are given by $f_{\text{CDW}} = 1$ and $f_{\text{PDW}} = i\sin k_{\parallel}$. These order parameters in real space are given by

$$O_{\text{CDW}} = 2\sum_{j,\sigma}(c^{\dagger}_{j,1,\sigma}c_{j,1,\sigma} - c^{\dagger}_{j,2,\sigma}c_{j,2,\sigma})\cos 2k_F R_j, \tag{2.9a}$$

$$O_{\text{PDW}} = \sum_{j,\sigma}(c^{\dagger}_{j-1,1,\sigma}c_{j,1,\sigma} - c^{\dagger}_{j-1,2,\sigma}c_{j,2,\sigma} - c^{\dagger}_{j,1,\sigma}c_{j+1,1,\sigma} + c^{\dagger}_{j,2,\sigma}c_{j+1,2,\sigma})\cos 2k_F R_j, \tag{2.9b}$$

where $R_j = ja$. The order parameter of the PDW state corresponds to that of the spin-Peierls state in the limit of $\delta \to 0$. One can also consider other density-wave states such as the $d$-density-wave state, the $f$-density-wave state, or another superconducting state with $s$-wave symmetry, which are known to span the finite parameter space of the ground-state phase diagram in the extended Hubbard ladder.[31,33] However, for the case of $U \gg V_{\parallel}$, $V_{\perp} > 0$, these unconventional states do not become dominant.

### A. $g$-ology

Following the standard weak-coupling approach ($g$-ology), we linearize the energy bands around the Fermi points. The linearized kinetic energy is given by

$$H_0 = \sum_{\boldsymbol{k},p,\sigma} v_F(pk_{\parallel} - k_{F,k_{\perp}})c^{\dagger}_{p,\sigma}(\boldsymbol{k})c_{p,\sigma}(\boldsymbol{k}), \tag{2.10}$$

where the index $p = +$ $(-)$ denotes the right- (left-)moving electron. We introduce field operators of the right- and left-

going electrons defined by $\psi_{p,\sigma,+}(x)=L^{-1/2}\Sigma_{k_\parallel}e^{ik_\parallel x}c_{p,\sigma}(k_\parallel,0)$ and $\psi_{p,\sigma,-}(x)=L^{-1/2}\Sigma_{k_\parallel}e^{ik_\parallel x}c_{p,\sigma}(k_\parallel,\pi)$ where $L$ is the length of the chains: $L=Na$.

The interactions near the Fermi points are written as $H_{\rm int}=\int dx\,\mathcal{H}_{\rm int}$, where

$$\begin{aligned}\mathcal{H}_{\rm int}=\frac{1}{4}\sum_{p,\sigma}\sum_{\zeta_i=\pm}{}'[&g_{1\parallel}^{\epsilon\bar{\epsilon}}\psi^\dagger_{p,\sigma,\zeta_1}\psi^\dagger_{-p,\sigma,\zeta_2}\psi_{p,\sigma,\zeta_4}\psi_{-p,\sigma,\zeta_3}\\&+g_{1\perp}^{\epsilon\bar{\epsilon}}\psi^\dagger_{p,\sigma,\zeta_1}\psi^\dagger_{-p,\bar{\sigma},\zeta_2}\psi_{p,\bar{\sigma},\zeta_4}\psi_{-p,\sigma,\zeta_3}\\&+g_{2\parallel}^{\epsilon\bar{\epsilon}}\psi^\dagger_{p,\sigma,\zeta_1}\psi^\dagger_{-p,\sigma,\zeta_2}\psi_{-p,\sigma,\zeta_4}\psi_{p,\sigma,\zeta_3}\\&+g_{2\perp}^{\epsilon\bar{\epsilon}}\psi^\dagger_{p,\sigma,\zeta_1}\psi^\dagger_{-p,\bar{\sigma},\zeta_2}\psi_{-p,\bar{\sigma},\zeta_4}\psi_{p,\sigma,\zeta_3}],\end{aligned}\tag{2.11}$$

where $\bar{\sigma}=\uparrow(\downarrow)$ for $\sigma=\downarrow(\uparrow)$ and $\epsilon\equiv\zeta_1\zeta_3$ and $\bar{\epsilon}\equiv\zeta_1\zeta_2$. The primed summation over $\zeta_i$ $(i=1,\ldots,4)$ is taken under the condition $\zeta_1\zeta_2\zeta_3\zeta_4=+1$, which comes from the momentum conservation in the transverse direction. Each $g^{\epsilon\bar{\epsilon}}$ has two different processes [e.g., for $g^{++}$ one has $(\zeta_1,\zeta_2,\zeta_3,\zeta_4)=(+,+,+,+)$ and $(-,-,-,-)$]; however, these two different processes are given in the same form in the bosonized Hamiltonian and contribute to physical quantities in the same manner, as will be shown later. Then the coupling constants $g_{i\parallel}^{\epsilon\bar{\epsilon}}$ and $g_{i\perp}^{\epsilon\bar{\epsilon}}$ are written in terms of interactions of the Hamiltonian (2.1) as

$$g_{i\parallel}^{\epsilon\bar{\epsilon}}=l_\epsilon V_\perp+m_{i,\epsilon}V_\parallel,\tag{2.12a}$$

$$g_{i\perp}^{\epsilon\bar{\epsilon}}=U+l_\epsilon V_\perp+m_{i,\epsilon}V_\parallel,\tag{2.12b}$$

where $l_\pm=\pm1$, $m_{1,+}=-2\cos\pi\delta\cos2\lambda$, $m_{1,-}=-2\cos\pi\delta$, $m_{2,+}=+2$, and $m_{2,-}=+2\cos2\lambda$.

### B. Bosonization

Here we apply the Abelian bosonization method.[35–37] The field operators of the right- and left-moving electrons are then written as

$$\psi_{p,\sigma,\zeta}(x)=\frac{\eta_{\sigma,\zeta}}{\sqrt{2\pi a}}\exp[ipk_{F,k_\perp}x+ip\varphi_{p,s,\zeta}(x)],\tag{2.13}$$

where $s=+(-)$ for $\sigma=\uparrow(\downarrow)$. The chiral bosons obey the commutation relations $[\varphi_{p,s,\zeta}(x),\varphi_{p,s',\zeta'}(x')]=ip\pi\,\mathrm{sgn}(x-x')\delta_{s,s'}\delta_{\zeta,\zeta'}$ and $[\varphi_{+,s,\zeta},\varphi_{-,s',\zeta'}]=i\pi\delta_{s,s'}\delta_{\zeta,\zeta'}$. The Klein factors $\eta_{\sigma,\zeta}$ are introduced in order to retain the correct anticommutation relations of the field operators between different spin and band indices. To relate the bosonic field $\varphi$ to the physical quantity, we introduce a new set of bosonic fields $\phi_{\rho\pm}$ and $\phi_{\sigma\pm}$ by

$$\phi^p_{\rho+}(x)=\frac{1}{4}\sum_{s,\zeta=\pm}\varphi_{p,s,\zeta}(x),\tag{2.14a}$$

$$\phi^p_{\rho-}(x)=\frac{1}{4}\sum_{s,\zeta=\pm}\zeta\varphi_{p,s,\zeta}(x),\tag{2.14b}$$

$$\phi^p_{\sigma+}(x)=\frac{1}{4}\sum_{s,\zeta=\pm}s\varphi_{p,s,\zeta}(x),\tag{2.14c}$$

$$\phi^p_{\sigma-}(x)=\frac{1}{4}\sum_{s,\zeta=\pm}s\zeta\varphi_{p,s,\zeta}(x).\tag{2.14d}$$

The phases $\phi_{\rho\pm}$ and $\phi_{\sigma\pm}$ represent charge and spin fluctuations, respectively, and the suffix + (−) refers to the even (odd) sector.

In terms of bosonic fields, we can rewrite the kinetic energy as $H_0=\int dx\,\mathcal{H}_0$, where

$$\mathcal{H}_0=\frac{v_F}{\pi}\sum_{\nu=\rho,\sigma}\sum_{r=\pm}[(\partial_x\phi^+_{\nu r})^2+(\partial_x\phi^-_{\nu r})^2].\tag{2.15}$$

We also introduce the field $\phi_{\nu r}$ and its dual field $\theta_{\nu r}$ defined by $\phi_{\nu r}=\phi^+_{\nu r}+\phi^-_{\nu r}$ and $\theta_{\nu r}=\phi^+_{\nu r}-\phi^-_{\nu r}$. These fields satisfy the commutation relation $[\phi_{\nu r}(x),\theta_{\nu' r'}(x')]=-i\pi\Theta(-x+x')\delta_{r,r'}$, where $\Theta(x)$ is the Heaviside step function.

In terms of these bosonic fields, the order parameters are expressed as $O_A=\int dx\,\mathcal{O}_A(x)$, where

$$\begin{aligned}\mathcal{O}_{\mathrm{SC}d}(x)&=\sum_{p,\zeta}\zeta\,\psi_{p,\uparrow,\zeta}(x)\psi_{-p,\downarrow,\zeta}(x)\\&\propto e^{i\theta_{\rho+}}\cos\theta_{\rho-}\cos\phi_{\sigma+}\cos\phi_{\sigma-}\\&\quad-ie^{i\theta_{\rho+}}\sin\theta_{\rho-}\sin\phi_{\sigma+}\sin\phi_{\sigma-},\end{aligned}\tag{2.16a}$$

$$\begin{aligned}\mathcal{O}_{\mathrm{CDW}}(x)&=\sum_{p,\sigma,\zeta}\psi^\dagger_{p,\sigma,\zeta}(x)\psi_{-p,\sigma,-\zeta}(x)e^{ip2k_Fx}\\&\propto\sin\phi_{\rho+}\cos\theta_{\rho-}\sin\phi_{\sigma+}\sin\theta_{\sigma-}\\&\quad-\cos\phi_{\rho+}\sin\theta_{\rho-}\cos\phi_{\sigma+}\cos\theta_{\sigma-},\end{aligned}\tag{2.16b}$$

$$\begin{aligned}\mathcal{O}_{\mathrm{PDW}}(x)&=\sum_{p,\sigma,\zeta}(ip)\psi^\dagger_{p,\sigma,\zeta}(x)\psi_{-p,\sigma,-\zeta}(x)e^{ip2k_Fx}\\&\propto\cos\phi_{\rho+}\cos\theta_{\rho-}\sin\phi_{\sigma+}\sin\theta_{\sigma-}\\&\quad+\sin\phi_{\rho+}\sin\theta_{\rho-}\cos\phi_{\sigma+}\cos\theta_{\sigma-}.\end{aligned}\tag{2.16c}$$

In the present paper we do not consider the $4k_F$ CDW order parameter. The possibility of the $4k_F$ CDW state will be discussed later in Sec. III.

To obtain the bosonized Hamiltonian, Eq. (2.13) is substituted for the interaction term Eq. (2.11). The phase field $\phi_{\rho-}$ appears in the form $\cos(2\phi_{\rho-}+4\lambda x)$ where $\lambda$ is given by Eq. (2.6). We can safely assume that $t_\perp$ is relevant for $t_\perp$ being not very small. In this case we can discard the $\cos(2\phi_{\rho-}+4\lambda x)$ terms which become irrelevant. We also neglect the $\cos2\phi_{\sigma-}\cos2\theta_{\sigma-}$ term, because this cannot become relevant due to the scaling dimension of $\cos2\phi_{\sigma-}\cos2\theta_{\sigma-}$ being equal to or larger than 2, i.e., this term is either marginal or irrelevant. Then our Hamiltonian reduces to

$$\begin{aligned}\mathcal{H}=&\frac{v_F}{\pi}\sum_{r=\pm}\left[\sum_{p=\pm}(\partial_x\phi^p_{\rho r})^2+\frac{g_{\rho r}}{\pi v_F}(\partial_x\phi^+_{\rho r})(\partial_x\phi^-_{\rho r})\right]\\&+\frac{v_F}{\pi}\sum_{r=\pm}\left[\sum_{p=\pm}(\partial_x\phi^p_{\sigma r})^2-\frac{g_{\sigma r}}{\pi v_F}(\partial_x\phi^+_{\sigma r})(\partial_x\phi^-_{\sigma r})\right]\\&+\frac{1}{2\pi^2a^2}[g^{--}_{c-,s+}\cos2\theta_{\rho-}\cos2\phi_{\sigma+}\end{aligned}$$

TABLE I. Position of phase locking and signs for the fixed-point coupling constants, which are essentially the same as in Ref. 31. The $*$ symbol indicates that a bosonic field is not locked. $I_i$ are integers.

| | $\langle\theta_{\rho-}\rangle$ | $\langle\phi_{\sigma+}\rangle$ | $\langle\phi_{\sigma-}\rangle$ | $\langle\theta_{\sigma-}\rangle$ | $(g^*_{\overline{c-},s+}, g^*_{\overline{c-},s-}, g^*_{\overline{c-},\overline{s-}}, g^*_{s+,s-}, g^*_{s+,\overline{s-}})$ |
|---|---|---|---|---|---|
| CDW+PDW | $(\pi/2)(I_0+1)+\pi I_1$ | $(\pi/2)I_0+\pi I_2$ | $*$ | $(\pi/2)I_0+\pi I_3$ | $(+,0,+,0,-)$ |
| SC$d$ | $(\pi/2)I_0+\pi I_1$ | $(\pi/2)I_0+\pi I_2$ | $(\pi/2)I_0+\pi I_3$ | $*$ | $(-,-,0,-,0)$ |

$$+ g_{\overline{c-},s-}\cos 2\theta_{\rho-}\cos 2\phi_{\sigma-} + g_{\overline{c-},\overline{s-}}\cos 2\theta_{\rho-}\cos 2\theta_{\sigma-} + g_{s+,s-}\cos 2\phi_{\sigma+}\cos 2\phi_{\sigma-} + g_{s+,\overline{s-}}\cos 2\phi_{\sigma+}\cos 2\theta_{\sigma-}]. \tag{2.17}$$

The coupling constants for the bilinear terms of the density operators are given by

$$g_{\rho+} = +\frac{1}{2}\sum_{\epsilon=\pm}(g_{2\parallel}^{+\epsilon} + g_{2\perp}^{+\epsilon} - g_{1\parallel}^{\epsilon\epsilon}), \tag{2.18a}$$

$$g_{\rho-} = +\frac{1}{2}\sum_{\epsilon=\pm}\epsilon(g_{2\parallel}^{+\epsilon} + g_{2\perp}^{+\epsilon} - g_{1\parallel}^{\epsilon\epsilon}), \tag{2.18b}$$

$$g_{\sigma+} = -\frac{1}{2}\sum_{\epsilon=\pm}(g_{2\parallel}^{+\epsilon} - g_{2\perp}^{+\epsilon} - g_{1\parallel}^{\epsilon\epsilon}), \tag{2.18c}$$

$$g_{\sigma-} = -\frac{1}{2}\sum_{\epsilon=\pm}\epsilon(g_{2\parallel}^{+\epsilon} - g_{2\perp}^{+\epsilon} - g_{1\parallel}^{\epsilon\epsilon}), \tag{2.18d}$$

and the coupling constants for the nonlinear terms are given by

$$g_{\overline{c-},s+} = -g_{1\perp}^{-+}, \tag{2.19a}$$

$$g_{\overline{c-},s-} = -g_{2\perp}^{-+}, \tag{2.19b}$$

$$g_{\overline{c-},\overline{s-}} = +g_{2\parallel}^{-+} - g_{1\parallel}^{-+}, \tag{2.19c}$$

$$g_{s+,s-} = +g_{1\perp}^{++}, \tag{2.19d}$$

$$g_{s+,\overline{s-}} = +g_{1\perp}^{--}. \tag{2.19e}$$

Since there is no cosine potential for the phase $\phi_{\rho+}$ in the Hamiltonian (2.17), the phase $\phi_{\rho+}$ is not locked even in the low-energy limit. Then the CDW state and the PDW state cannot be distinguished. Actually, by the translation of the phase $\phi_{\rho+}\to\phi_{\rho+}+\pi/2$, the order parameters $\mathcal{O}_{\mathrm{CDW}}$ [Eq. (2.16b)] and $\mathcal{O}_{\mathrm{PDW}}$ [Eq. (2.16c)] are interchanged, while the Hamiltonian (2.17) is invariant. Thus if the CDW state becomes (quasi-)long-range ordered, the PDW state also becomes so, and then these two states coexist: We call this coexisting state the CDW+PDW state.

From Eqs. (2.16) and (2.17), the CDW+PDW state and SC$d$ state are identified by the fixed points of $g$s as summarized in Table I. Both states have a gap in the total spin sector $\phi_{\sigma+}$. The first reason, attributable to the difference between the CDW+PDW state and the SC$d$ state, is that of the locking position for the $\theta_{\rho-}$ mode and the $\phi_{\sigma+}$ mode, where the solution $g^*_{\overline{c-},s+}<0$ leads to $\langle\theta_{\rho-}\rangle=\langle\phi_{\sigma+}\rangle=0$ or $\pi/2$ for the SC$d$ state, and the solution $g^*_{\overline{c-},s+}>0$ results in $\langle\theta_{\rho-}\rangle \neq \langle\phi_{\sigma+}\rangle$ for the CDW+PDW state. The second reason is the relevance of $\phi_{\sigma-}$ or $\theta_{\sigma-}$: The CDW+PDW state is obtained for the locking of $\theta_{\sigma-}$ due to the relevant $g^*_{\overline{c-},\overline{s-}}$ and $g^*_{s+,\overline{s-}}$ terms, while the SC$d$ state is obtained for that of $\phi_{\sigma-}$ due to the relevant $g^*_{\overline{c-},s-}$ and $g^*_{s+,s-}$ terms.

### C. Refermionization and effective theory for spin modes

The coupling constants in Eq. (2.11) are not independent parameters due to the global spin-rotation SU(2) symmetry. In terms of the coupling constants in Eq. (2.17), the constraint is given by[33,38]

$$g_{\sigma+} + g_{\sigma-} - g_{s+,s-} = 0, \tag{2.20a}$$

$$g_{\sigma+} - g_{\sigma-} - g_{s+,\overline{s-}} = 0, \tag{2.20b}$$

$$g_{\overline{c-},s+} - g_{\overline{c-},s-} - g_{\overline{c-},\overline{s-}} = 0. \tag{2.20c}$$

Since the SU(2) symmetry holds in the original Hubbard Hamiltonian (2.1), the coupling constants in Eq. (2.17) must satisfy Eq. (2.20) in the course of renormalization.

To appreciate the SU(2) symmetry in the effective theory (2.17), we fermionize it by introducing spinless fermion fields $\psi_{p,r}$ ($p=\pm$ and $r=\pm$):

$$\psi_{\pm,r}(x) = \frac{\eta_r}{\sqrt{2\pi a}}\exp[\pm i2\phi_{\sigma r}^{\pm}(x)], \tag{2.21}$$

where the index $r=+$ $(-)$ refers to the total (relative) degrees of freedom of the spin mode, and $\{\eta_r,\eta_{r'}\}=2\delta_{r,r'}$. The density operators are given by $\psi^\dagger_{p,\pm}\psi_{p,\pm} := \partial_x\phi^p_{\sigma\pm}/\pi$. We then introduce the Majorana fermions $\xi^n$ $(n=1$–$4)$ by

$$\psi_{p,+} = \frac{1}{\sqrt{2}}(\xi_p^2 + i\xi_p^1), \quad \psi_{p,-} = \frac{1}{\sqrt{2}}(\xi_p^4 + i\xi_p^3). \tag{2.22}$$

These fields satisfy the anticommutation relations $\{\xi_p^n(x),\xi_{p'}^{n'}(x')\}=\delta(x-x')\delta_{p,p'}\delta_{n,n'}$. With the help of the SU(2) constraints (2.20), we rewrite the effective Hamiltonian (2.17) in terms of the Majorana fermions:

$$\mathcal{H} = \frac{v_F}{\pi}\sum_r\left[\sum_p(\partial\phi_{\rho r}^p)^2 + \frac{g_{\rho r}}{\pi v_F}(\partial_x\phi_{\rho r}^+)(\partial_x\phi_{\rho r}^-)\right] - i\frac{v_F}{2}(\boldsymbol{\xi}_+\cdot\partial_x\boldsymbol{\xi}_+ - \boldsymbol{\xi}_-\cdot\partial_x\boldsymbol{\xi}_-) - \frac{g_{\sigma+}}{2}(\boldsymbol{\xi}_+\cdot\boldsymbol{\xi}_-)^2 - i\frac{v_F}{2}(\xi_+^4\partial_x\xi_+^4 - \xi_-^4\partial_x\xi_-^4) - i\frac{g_{\overline{c-},st}}{2\pi a}\cos 2\theta_{\rho-}\boldsymbol{\xi}_+\cdot\boldsymbol{\xi}_-$$

$$-i\frac{g_{\overline{c-},ss}}{2\pi a}\cos 2\theta_{\rho-}\xi_+^4\cdot\xi_-^4 - g_{\sigma-}(\boldsymbol{\xi}_+\cdot\boldsymbol{\xi}_-)\xi_+^4\xi_-^4, \quad (2.23)$$

where $\boldsymbol{\xi}_p=(\xi_p^1,\xi_p^2,\xi_p^3)$, and the coupling constants are

$$g_{\overline{c-},st} \equiv -g_{\overline{c-},s+}, \quad g_{\overline{c-},ss} \equiv -g_{\overline{c-},s-}+g_{\overline{c-},\overline{s-}}. \quad (2.24)$$

These coupling constants are given in terms of the Hubbard interactions as

$$g_{\overline{c-},st} = +U - V_\perp - 2V_\parallel\cos\pi\delta, \quad (2.25a)$$

$$g_{\overline{c-},ss} = +U - V_\perp + 2V_\parallel(\cos\pi\delta + 2\cos 2\lambda), \quad (2.25b)$$

$$g_{\rho+} = +U + 2V_\perp + V_\parallel[4+\cos\pi\delta(1+\cos 2\lambda)], \quad (2.25c)$$

$$g_{\rho-} = -V_\perp - V_\parallel\cos\pi\delta(1-\cos 2\lambda), \quad (2.25d)$$

$$g_{\sigma+} = +U - V_\parallel\cos\pi\delta(1+\cos 2\lambda), \quad (2.25e)$$

$$g_{\sigma-} = +V_\perp + V_\parallel\cos\pi\delta(1-\cos 2\lambda). \quad (2.25f)$$

Thus the effective theory for the spin sector becomes O(3) $\times Z_2$ symmetric, i.e., the four Majorana fermions are grouped into a singlet $\xi^4$ and a triplet $\boldsymbol{\xi}$. We note that the $O(3)\times Z_2$ symmetry also appears in the low-energy effective theory of the isotropic Heisenberg ladder.[39]

## III. PHASE DIAGRAM IN THE GROUND STATE

We investigate the low-energy behavior using perturbative RG analysis. There are six independent RG equations for the scaling of the coupling constants under the transformation of the lattice constant $a\to ae^{dl}$. From Eq. (2.23), we obtain the RG equations

$$\frac{d}{dl}G_{\rho-} = -\frac{3}{4}G_{\overline{c-},st}^2 - \frac{1}{4}G_{\overline{c-},ss}^2, \quad (3.1a)$$

$$\frac{d}{dl}G_{\sigma+} = -G_{\sigma+}^2 - G_{\sigma-}^2 - \frac{1}{2}G_{\overline{c-},st}^2, \quad (3.1b)$$

$$\frac{d}{dl}G_{\sigma-} = -2G_{\sigma+}G_{\sigma-} - \frac{1}{2}G_{\overline{c-},st}G_{\overline{c-}ss}, \quad (3.1c)$$

$$\frac{d}{dl}G_{\overline{c-},st} = -G_{\rho-}G_{\overline{c-},st} - 2G_{\sigma+}G_{\overline{c-},st} - G_{\sigma-}G_{\overline{c-},ss}, \quad (3.1d)$$

$$\frac{d}{dl}G_{\overline{c-},ss} = -G_{\rho-}G_{\overline{c-},ss} - 3G_{\sigma-}G_{\overline{c-},st}, \quad (3.1e)$$

and $dG_{\rho+}/dl=0$ where $G(0)=g/(2\pi v_F)$. Note that these RG equations can also be derived directly from Eqs. (2.17) and (2.20). Since the coupling $G_{\rho+}$ is unchanged under renormalization, the total charge sector is critical and has gapless excitations. The asymptotic behavior of these coupling constants for large $l$ is examined by integrating the RG equations (3.1) numerically with the initial conditions (2.25). It is easily found that, in most cases, all the coupling constants in Eq. (3.1) grow under renormalization and become relevant at large $l$. This fact implies that all the modes except for the $\phi_{\rho+}$ mode become massive in most regions of the ground-state phase diagram.[28,29,40] These stable fixed points are called the "C1S0 phase," where the notation C$n$S$m$ denotes $n$ massless boson modes in the charge sector and $m$ massless boson modes in the spin sector.[29] The characteristic energy scale corresponding to the mass gap can be roughly estimated from $|m_a|=\Lambda e^{-l_a}$ where $\Lambda$ is the high-energy cutoff of the order of the bandwidth and $l_a$ is determined by using the fact that the corresponding coupling constant $|G_a(l)|$ becomes of the order of unity at $l=l_a$.

From Eq. (3.1), we also find that there are two distinct stable fixed points on the plane of the coupling constants for the original extended Hubbard ladder model with $U$ ($>0$), $V_\parallel$ ($\geqslant 0$), and $V_\perp$ ($\geqslant 0$). Actually, from Table I, one obtains that the coupling constants $(G_{\rho-},G_{\sigma+},G_{\sigma-},G_{\overline{c-},st},G_{\overline{c-},ss})$ flow to $(-,-,+,-,+)$ for the CDW+PDW state and $(-,-,-,+,+)$ for the SC$d$ state. This means that there are two distinct phases in the ground states of the extended Hubbard ladder model, and that the system exhibits a quantum phase transition on a critical point between two phases. In order to examine critical properties in the ground state, we analyze Eq. (2.23) in more detail by deriving the effective theory for low-energy properties.

Here we assume that the mass of the charge mode of odd sector ($\rho-$) is larger than those of the spin modes ($\sigma\pm$), so that the $\theta_{\rho-}$ fields are locked by cosine potential below the scale of the mass $m_{\rho-}$. This assumption will be examined later. The effective low-energy theory is obtained from Eq. (2.17) by taking an average:

$$c_{\overline{\rho-}} \equiv \langle\cos 2\theta_{\rho-}\rangle. \quad (3.2)$$

Then we have

$$\mathcal{H}_\sigma = -i\frac{v_F}{2}(\boldsymbol{\xi}_+\cdot\partial_x\boldsymbol{\xi}_+ - \boldsymbol{\xi}_-\cdot\partial_x\boldsymbol{\xi}_-) - im_t^0\boldsymbol{\xi}_+\cdot\boldsymbol{\xi}_- - i\frac{v_F}{2}(\xi_+^4\partial_x\xi_+^4 - \xi_-^4\partial_x\xi_-^4) - im_s^0\xi_+^4\xi_-^4 - \frac{g_{\sigma+}}{2}(\boldsymbol{\xi}_+\cdot\boldsymbol{\xi}_-)^2 - g_{\sigma-}(\boldsymbol{\xi}_+\cdot\boldsymbol{\xi}_-)\xi_+^4\xi_-^4, \quad (3.3)$$

where we have introduced

$$m_t^0 \equiv \frac{c_{\overline{\rho-}}}{2\pi a}g_{\overline{c-},st}, \quad m_s^0 \equiv \frac{c_{\overline{\rho-}}}{2\pi a}g_{\overline{c-},ss}. \quad (3.4)$$

Such a mean-field treatment of the charge sector has also been utilized in the context of carbon nanotubes.[41] We note that this low-energy effective theory takes the same form as that of the isotropic Heisenberg ladder.[39] In terms of the original Hubbard interactions these masses of Eq. (3.4) are given by

$$m_t^0 = \frac{c_{\overline{\rho-}}}{2\pi a}[U - V_\perp - 2V_\parallel \cos \pi\delta], \tag{3.5a}$$

$$m_s^0 = \frac{c_{\overline{\rho-}}}{2\pi a}[U - V_\perp + 2V_\parallel(\cos \pi\delta + 2\cos 2\lambda)]. \tag{3.5b}$$

Thus the magnitude of the masses can be tuned by the interactions and doping. It is known that, when $m_s^0$, $m_t^0 \neq 0$, the quartic marginal terms lead to mass renormalization, $m_s^0 \to m_s$ and $m_t^0 \to m_t$, where[37,39]

$$m_t = m_t^0 - \frac{g_{\sigma+}}{\pi v_F} m_t^0 \ln\frac{\Lambda}{|m_t^0|} - \frac{g_{\sigma-}}{2\pi v_F} m_s^0 \ln\frac{\Lambda}{|m_s^0|}, \tag{3.6a}$$

$$m_s = m_s^0 - \frac{3g_{\sigma-}}{2\pi v_F} m_t^0 \ln\frac{\Lambda}{|m_t^0|}, \tag{3.6b}$$

and $\Lambda$ is a high-energy cutoff. Then Eq. (3.3) reduces to

$$\mathcal{H}_\sigma = -i\frac{v_F}{2}(\boldsymbol{\xi}_+ \cdot \partial_x \boldsymbol{\xi}_+ - \boldsymbol{\xi}_- \cdot \partial_x \boldsymbol{\xi}_-) - im_t \boldsymbol{\xi}_+ \cdot \boldsymbol{\xi}_- - i\frac{v_F}{2}(\xi_+^4 \partial_x \xi_+^4 - \xi_-^4 \partial_x \xi_-^4) - im_s \xi_+^4 \xi_-^4. \tag{3.7}$$

Low-energy properties become more transparent by introducing four copies of the one-dimensional quantum Ising model:

$$H_{\mathrm{QI}} = -\sum_j \sum_l (J\sigma_{j,l}^z \sigma_{j+1,l}^z + h_l \sigma_{j,l}^x), \tag{3.8}$$

where $\sigma_j^z$ and $\sigma_j^x$ are the Pauli matrices and $l=1, 2, 3, 4$. This model is equivalent to the Majorana-fermion theory with the central charge $c=1/2$. The operator $\mu$, being dual to the spin operator $\sigma$, is defined as[37]

$$\mu_{j+1/2,l}^z = \prod_{i=1}^{j} \sigma_{i,l}^x, \quad \mu_{j+1/2,l}^x = \sigma_{j,l}^z \sigma_{j+1,l}^z, \tag{3.9}$$

which is known as the Kramers-Wannier transformation in the one-dimensional quantum Ising model. These variables satisfy $[\sigma_{i,l}^z, \mu_{j+1/2,l}^z] = 0$ for $i > j$ and $\{\sigma_{i,l}^z, \mu_{j+1/2,l}^z\} = 0$ for $i \leqslant j$. In terms of $\sigma^z$ and $\mu^z$, i.e., the Ising order and disorder parameters, the Majorana fermions can be constructed as

$$\eta_{j,l} = \kappa_l \sigma_{j,l}^z \mu_{j-1/2,l}^z, \quad \zeta_{j,l} = i\kappa_l \sigma_{j,l}^z \mu_{j+1/2,l}^z, \tag{3.10}$$

where $\kappa_l$ is the Klein factor. One can easily check the anticommutation relation of the Majorana fermions, $\{\eta_{i,l}, \eta_{j,m}\} = \{\zeta_{i,l}, \zeta_{j,m}\} = 2\delta_{i,j}\delta_{l,m}$ and $\{\eta_{i,l}, \zeta_{j,m}\} = 0$. By using $\xi_+^l = (-\eta_l + \zeta_l)/\sqrt{2}$ and $\xi_-^l = (\eta_l + \zeta_l)/\sqrt{2}$, and by taking the continuum limit, the quantum Ising Hamiltonian Eq. (3.8) reproduces Eq. (3.7) where $v_F = 2J$, $m_t = 2(h_1 - J)$, and $m_s = 2(h_4 - J)$ with $h_1 = h_2 = h_3$. It is well known that the Ising model (3.8) exhibits a quantum critical point at $h_l = J$.[42] For $h_l < J$, the ordered state is obtained, i.e., the order parameter $\sigma_l$ has a finite expectation value. For $h_l > J$, on the other hand, we have the disordered state where the expectation value of $\sigma_l$ becomes zero, while the disorder parameter $\mu_l$ has a finite expectation value. On the critical point $h_l = J$, the corresponding mass in Eq. (3.7) vanishes with its central charge $c = \frac{1}{2}$ for each Ising chain.[43] Thus the ground-state properties are determined from the sign of masses $m_t$ and $m_s$. When $m_t < 0$, i.e., the Ising model with $l = 1, 2, 3$ is in the ordered phase, we have $\langle\sigma_1\rangle = \langle\sigma_2\rangle = \langle\sigma_3\rangle \neq 0$ and $\langle\mu_1\rangle = \langle\mu_2\rangle = \langle\mu_3\rangle = 0$, and vice versa. In the same manner, we have $\langle\sigma_4\rangle \neq 0$ and $\langle\mu_4\rangle = 0$ for $m_s < 0$, while $\langle\sigma_4\rangle = 0$ and $\langle\mu_4\rangle \neq 0$ for $m_s > 0$. In terms of the Ising variables, the order parameters Eq. (2.16) are rewritten as

TABLE II. Possible phases and related quantities: the signs of masses ($m_t$ and $m_s$) and order parameters. We have assumed $c_{\overline{\rho-}} \equiv \langle\theta_{\rho-}\rangle = 0 \bmod \pi$ in Eq. (3.4).

| | $m_t$ | $m_s$ | Order parameters |
|---|---|---|---|
| CDW+PDW | − | + | $\langle\sigma_{1,2,3}\rangle \neq 0$, $\langle\mu_4\rangle \neq 0$ |
| SC$d$ | + | + | $\langle\mu_{1,2,3}\rangle \neq 0$, $\langle\mu_4\rangle \neq 0$ |

$$\mathcal{O}_{\mathrm{SC}d} \propto e^{i\theta_{\rho+}}(\mu_1\mu_2\mu_3)\mu_4, \tag{3.11a}$$

$$\mathcal{O}_{\mathrm{CDW}} \propto \sin\phi_{\rho+}(\sigma_1\sigma_2\sigma_3)\mu_4, \tag{3.11b}$$

$$\mathcal{O}_{\mathrm{PDW}} \propto \cos\phi_{\rho+}(\sigma_1\sigma_2\sigma_3)\mu_4. \tag{3.11c}$$

As noted in the preceding section, we find that both the CDW and PDW states have the same structure for the spin degrees of freedom, since the field $\phi_{\rho+}$ is unlocked due to the doping effect. When $m_t < 0$ and $m_s > 0$, the CDW+PDW state becomes quasi-long-range ordered. In the case $m_t > 0$ and $m_s > 0$, the dominant fluctuation is the SC$d$ state, which is called the "Luther-Emery liquid."[44,45] The possible ground states and those order parameters are summarized in Table II.

Let us examine the behavior in more detail using the scaling equations for the coupling constants in the effective Hamiltonian (3.3). The scaling equations for the coupling constants are given by[33]

$$\frac{dM_t}{dl} = M_t - 2M_t G_{\sigma+} - M_s G_{\sigma-}, \tag{3.12a}$$

$$\frac{dM_s}{dl} = M_s - 3M_t G_{\sigma-}, \tag{3.12b}$$

$$\frac{dG_{\sigma+}}{dl} = -G_{\sigma+}^2 - G_{\sigma-}^2 - M_t^2, \tag{3.12c}$$

$$\frac{dG_{\sigma-}}{dl} = -2G_{\sigma+}G_{\sigma-} - M_t M_s, \tag{3.12d}$$

where $dl = da/a$, $M_t = m_t^0 a/v_F$, $M_s = m_s^0 a/v_F$, and $G_{\sigma\pm} = g_{\sigma\pm}/2\pi v_F$. The couplings $M_t$ and $M_s$ are relevant, while $G_{\sigma\pm}$ are marginal. These RG equations, which are analyzed in a way similar to Ref. 33, have two kinds of stable fixed point $M_t^* = \pm\infty$. The ground-state phase diagram, which is summarized in Table II, is shown in Fig. 1 on the plane of $U/t$ and $V/t$ ($t_\parallel = t_\perp \equiv t$, $V_\parallel = V_\perp \equiv V$). The SC$d$ quasi-long-range-ordered state, which is obtained for $V = 0$, is destabi-

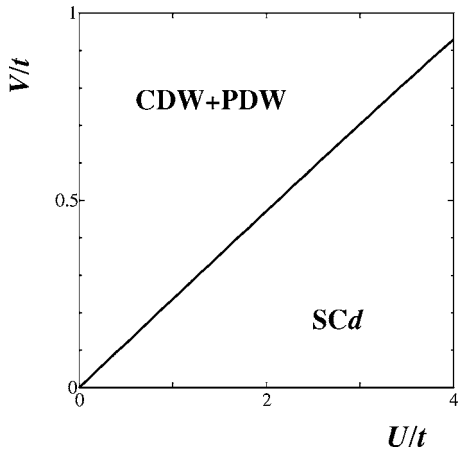


FIG. 1. The ground-state phase diagram on the plane of $U/t$ and $V/t$ where $t \equiv t_\perp = t_\parallel$ and $\delta = 0.2$.

lized by the intersite Coulomb repulsion and changes into the CDW+PDW state. The ground-state phase diagram on the plane of the doping $\delta$ and the ratio $V/U$ is shown in Fig. 2, where the SC$d$ state is stabilized due to the suppression of the intersite repulsion by the doping.

Here we discuss the possibility of the $4k_F$ CDW state. It is known that the $4k_F$ CDW state also becomes quasi-long-range ordered in the whole region of the phase diagrams, Figures 1 and 2, since the correlation function $4k_F$ CDW state decays[27,28] as $1/r^{2K_{\rho+}}$ where $K_{\rho+}$ is the Tomonaga-Luttinger parameter for the total charge sector, $K_{\rho+} \equiv [(2\pi v_F - g_{\rho+})/(2\pi v_F + g_{\rho+})]^{1/2}$. Since the correlation function of the CDW and PDW states decays as $1/r^{K_{\rho+}/2}$, we find that the $4k_F$ CDW state is still a subdominant fluctuation in the CDW+PDW state. On the other hand, in the SC$d$ state, the $4k_F$ CDW can become the dominant fluctuation for $K_{\rho+} < 1/2$, since the exponent of the SC$d$ correlation function is given by $1/2K_{\rho+}$. However, at close to half filling, it has been confirmed that the exponent $K_{\rho+}$ in ladder systems reaches a universal value $K^*_{\rho+} \to 1$ as $\delta \to 0$.[46–48] Thus in the SC$d$ state of the phase diagram, we find that the correlation function of the SC$d$ state becomes dominant and that of the $4k_F$ CDW state is subdominant close to half filling.

The doping dependences of the gaps,[49] which are roughly estimated from $|m_a| = \Lambda e^{-l_a}$, are shown in Fig. 3. The Majorana triplet gap $m_t$ collapses on the boundary between the CDW+PDW state and the SC$d$ state where the system is strongly fluctuating due to the competition between these two states. From the perturbative RG method, we cannot determine the precise magnitude of the gaps; however, the qualitative features of the gap associated with the phase transition (i.e., $m_t$ in the present case) can be captured close to the quantum critical point (QCP). The critical properties are described by the $SU(2)_2$ Wess-Zumino-Novikov-Witten (WZNW) model[37,39,50,51] and is also characterized by the $C1S\frac{3}{2}$ state.[28] In the present analysis, we have assumed $m_{\rho-} > (m_s, |m_t|)$ to derive the effective low-energy theory Eq. (3.3). Actually, by using Eq. (3.1), we find that $m_{\rho-}$ becomes the largest among the three $m_{\rho-}$, $m_t$, and $m_s$. However, $m_{\rho-}$ is not much larger than the Majorana singlet gap $m_s$, but is of the same order as $m_s$; we find from the above rough estimation that $m_{\rho-}/m_s \approx 1.4$–$1.6$ for $\delta = 0.1$–$0.4$. From the recent theoretical studies on the multicomponent one-dimensional systems, it has been proposed that[52–54] a symmetry, which is broken even in the microscopic Hamiltonian, can be restored nontrivially at low energies, due to coupling terms between different modes. This mechanism is called a dynamical symmetry enlargement (DSE) whose possibility has also been examined by the nonperturbative approach.[54] Once the DSE is realized, the resultant gaps for different modes become identical. Based on these theories, the present results with $m_{\rho-} \approx m_s$ may suggest the occurrence of the DSE between the charge sector $(\rho-)$ and the Majorana singlet sector where excitations form an O(3) multiplet. However, the study of the DSE is beyond the naive perturbative RG approach[52] and thus the DSE in the present case remains unclear.

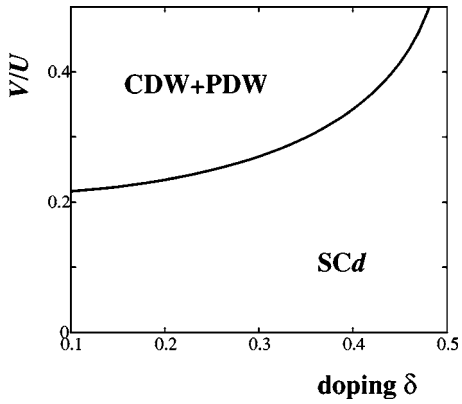


FIG. 2. The ground-state phase diagram on the plane of doping rate $\delta$ and ratio $V/U$ where $V \equiv V_\parallel = V_\perp$ and $U/t = 3$ with $t \equiv t_\perp = t_\parallel$.

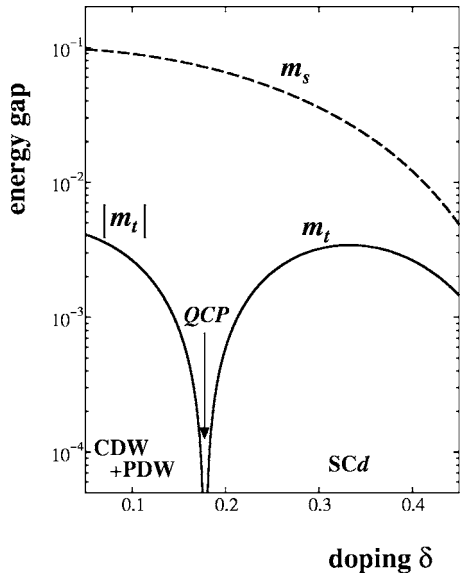


FIG. 3. The doping dependence of the energy gaps $m_t$ and $m_s$ with $U/t = 3$, $V_\parallel/t = V_\perp/t = 0.7$, and $t = t_\parallel = t_\perp = 1$. The quantum critical point (QCP) is at $\delta = \delta_c \approx 0.18$. The CDW+PDW quasi-long-range-ordered state is obtained for $\delta < \delta_c$, while the the $d$-wave SC quasi-long-range-ordered state is obtained for $\delta > \delta_c$.

## IV. SPIN SUSCEPTIBILITY AND NMR RELAXATION RATE

In this section we study the uniform spin susceptibility and the NMR relaxation rate at finite temperature from two different approaches by extending previous calculations on the single chain[55,56] or on the undoped Heisenberg ladder.[57–60] One approach is the random-phase approximation (RPA) combined with the renormalization group method and another is direct calculation in terms of the low-energy effective Hamiltonian (3.7). The former has the advantage of reproducing high-temperature behavior, while the latter is appropriate for describing the low-temperature asymptotics.

First we introduce the spin-$\frac{1}{2}$ operator:

$$\boldsymbol{S}(\boldsymbol{q}) \equiv \frac{1}{2}\sum_{\boldsymbol{k},\sigma_1,\sigma_2} c^{\dagger}_{\sigma_1}(\boldsymbol{k}+\boldsymbol{q})\boldsymbol{\sigma}_{\sigma_1,\sigma_2}c_{\sigma_2}(\boldsymbol{k}), \tag{4.1}$$

with $\boldsymbol{q}=(q_{\parallel},q_{\perp})$ and the Pauli matrices $\boldsymbol{\sigma}_{\sigma_1,\sigma_2}$. The generalized spin susceptibility is given by

$$\chi(\boldsymbol{q},i\omega_n) \equiv \frac{1}{2L}\int_0^{\beta} d\tau\langle T_{\tau}S^{\alpha}(\boldsymbol{q},\tau)S^{\alpha}(-\boldsymbol{q},0)\rangle e^{i\omega_n\tau}. \tag{4.2}$$

Equation (4.2) is independent of $\alpha$ due to the spin-rotational SU(2) symmetry, where $\alpha$ stands for the orientation of the magnetic field. The noninteracting susceptibility [i.e., Eq. (4.2) without interactions] is given by

$$\chi_0(\boldsymbol{q},i\omega_n) = \frac{1}{4L}\sum_{k_{\parallel},k_{\perp}} \frac{f(\varepsilon(\boldsymbol{k}+\boldsymbol{q}))-f(\varepsilon(\boldsymbol{k}))}{i\omega_n+\varepsilon(\boldsymbol{k})-\varepsilon(\boldsymbol{k}+\boldsymbol{q})}, \tag{4.3}$$

where $f(\varepsilon)$ is the Fermi distribution function $f(\varepsilon)=1/[e^{\beta(\varepsilon-\mu)}+1]$, and $\omega_n$ and $\mu$ are the Matsubara frequency and the chemical potential, respectively. In the continuum limit, we can split the spin operator into a uniform part varying slowly in space and a staggered oscillation part, as

$$\boldsymbol{S}(x,q_{\perp}) = \boldsymbol{J}_r(x) + (-1)^{x/a}\boldsymbol{n}_r(x), \tag{4.4}$$

where $r=+$ $(-)$ for $q_{\perp}=0$ $(\pi)$. The uniform part $(q_{\parallel}\approx 0)$ of the spin operator is given by

$$\boldsymbol{J}_+(x) = \frac{1}{2}\sum_{p,\zeta}\sum_{\sigma_1,\sigma_2}\psi^{\dagger}_{p,\sigma_1,\zeta}(x)\boldsymbol{\sigma}_{\sigma_1,\sigma_2}\psi_{p,\sigma_2,\zeta}(x), \tag{4.5a}$$

$$\boldsymbol{J}_-(x) = \frac{1}{2}\sum_{p,\zeta}\sum_{\sigma_1,\sigma_2}\psi^{\dagger}_{p,\sigma_1,\zeta}(x)\boldsymbol{\sigma}_{\sigma_1,\sigma_2}\psi_{p,\sigma_2,-\zeta}(x), \tag{4.5b}$$

where $\psi_{p,\sigma,\zeta}(x)$ is given by Eq. (2.13). By using Eqs. (2.13), (2.21), and (2.22), the spin operator $\boldsymbol{J}_{\pm}(x)$ is expressed in terms of the Majorana fermions as

$$\boldsymbol{J}_+(x) = +\frac{i}{2}\sum_p \boldsymbol{\xi}_p(x)\times\boldsymbol{\xi}_p(x), \tag{4.6a}$$

$$\boldsymbol{J}_-(x) = -i\sum_p \boldsymbol{\xi}_p(x)\xi^4_p(x), \tag{4.6b}$$

where $\boldsymbol{J}_{\pm}=(J^x_{\pm},J^y_{\pm},J^z_{\pm})=(J^1_{\pm},J^2_{\pm},J^3_{\pm})$. The staggered part $(q_{\parallel}\approx 2k_F$ and $q_{\perp}=\pi)$ of the spin operator is given by

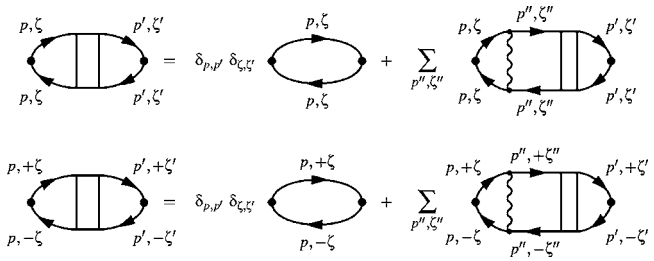


FIG. 4. The spin susceptibility $\chi(q_{\parallel},q_{\perp},\omega)$ with $q_{\perp}=0$ (upper diagram) and $\pi$ (lower diagram), and small $q_{\parallel}$. The subscript $p=+$ $(-)$ refers to right- (left-)moving electrons, while $\zeta=+$ $(-)$ refers to electrons on the bonding (antibonding) band.

$$\boldsymbol{n}_-(x) = \frac{(-1)^{x/a}}{2}\sum_{p,\zeta}\sum_{\sigma_1,\sigma_2}\psi^{\dagger}_{p,\sigma_1,\zeta}(x)\boldsymbol{\sigma}_{\sigma_1,\sigma_2}\psi_{-p,\sigma_2,-\zeta}(x). \tag{4.7}$$

Here we do not consider the component with $(q_{\parallel},q_{\perp})\approx(2k_F,0)$, which would become irrelevant in the low-energy limit due to the relevant $t_{\perp}$.[61] By using Eq. (2.13), the operator $\boldsymbol{n}_-$ is rewritten as

$$n^x_-(x) = \frac{-2i}{\pi a}(\cos\tilde{\phi}_{\rho+}\cos\theta_{\rho-}\sin\theta_{\sigma+}\cos\phi_{\sigma-} - \sin\tilde{\phi}_{\rho+}\sin\theta_{\rho-}\cos\theta_{\sigma+}\sin\phi_{\sigma-}), \tag{4.8a}$$

$$n^y_-(x) = \frac{-2i}{\pi a}(\cos\tilde{\phi}_{\rho+}\cos\theta_{\rho-}\cos\theta_{\sigma+}\cos\phi_{\sigma-} + \sin\tilde{\phi}_{\rho+}\sin\theta_{\rho-}\sin\theta_{\sigma+}\sin\phi_{\sigma-}), \tag{4.8b}$$

$$n^z_-(x) = \frac{2}{\pi a}(\cos\tilde{\phi}_{\rho+}\cos\theta_{\rho-}\cos\phi_{\sigma+}\sin\theta_{\sigma-} - \sin\tilde{\phi}_{\rho+}\sin\theta_{\rho-}\sin\phi_{\sigma+}\cos\theta_{\sigma-}), \tag{4.8c}$$

where $\tilde{\phi}_{\rho+}=\phi_{\rho+}-\pi\delta x$. Here we note that $\boldsymbol{n}_-(x)$ expresses the incommensurate spin-density wave.

### A. Uniform spin susceptibility

Here we calculate the uniform spin susceptibility. In terms of the spin operators $\boldsymbol{J}_{\pm}$, the spin susceptibility $\chi(\boldsymbol{q},i\omega_n)$ for small $q_{\parallel}$ is given by

$$\chi_{\mathrm{uni}}(\boldsymbol{q},i\omega_n) \equiv \frac{1}{2L}\int_0^{\beta} d\tau\langle T_{\tau}J^{\alpha}_r(q_{\parallel},\tau)J^{\alpha}_r(-q_{\parallel},0)\rangle e^{i\omega_n\tau}, \tag{4.9}$$

where $r=+(-)$ in the right-hand side (RHS) corresponds to $q_{\perp}=0(\pi)$ in the LHS and $\alpha$ denotes the orientation of the magnetic field. First we calculate $\chi_{\mathrm{uni}}(\boldsymbol{q},i\omega_n)$ within the RPA by using the formulation of $g$-ology (2.11). The magnetic susceptibility $\chi(q_{\parallel},q_{\perp},i\omega_n)$ for small $q_{\parallel}$ is calculated from the diagrams of the RPA given in Fig. 4. We note that the same result would be derived from the path integral formalism.[56] The explicit forms for the susceptibility are given by

$$\chi_{\rm uni}(q_\parallel,0,i\omega_n)=\frac{[\chi_0^+(q_\parallel,0,i\omega_n)+\chi_0^-(q_\parallel,0,i\omega_n)]+2(g_{1\perp}^{++}+g_{1\perp}^{--})\chi_0^+(q_\parallel,0,i\omega_n)\chi_0^-(q_\parallel,0,i\omega_n)}{1-(g_{1\perp}^{++}+g_{1\perp}^{--})^2\chi_0^+(q_\parallel,0,i\omega_n)\chi_0^-(q_\parallel,0,i\omega_n)}, \tag{4.10a}$$

$$\chi_{\rm uni}(q_\parallel,\pi,i\omega_n)=\frac{[\chi_0^+(q_\parallel,\pi,i\omega_n)+\chi_0^-(q_\parallel,\pi,i\omega_n)]+2(g_{1\perp}^{+-}+g_{1\perp}^{-+})\chi_0^+(q_\parallel,\pi,i\omega_n)\chi_0^-(q_\parallel,\pi,i\omega_n)}{1-(g_{1\perp}^{+-}+g_{1\perp}^{-+})^2\chi_0^+(q_\parallel,\pi,i\omega_n)\chi_0^-(q_\parallel,\pi,i\omega_n)}, \tag{4.10b}$$

where $\chi_0^p(q_\parallel,q_\perp,i\omega_n)$ is given by the noninteracting spin susceptibility per branch $p=+$ $(-)$:

$$\chi_0^p(\boldsymbol{q},i\omega_n)\equiv\frac{1}{4L}\sum_{k_\parallel\approx pk_F}\sum_{k_\perp}\frac{f(\varepsilon(\boldsymbol{k}+\boldsymbol{q}))-f(\varepsilon(\boldsymbol{k}))}{i\omega_n+\varepsilon(\mathbf{k})-\varepsilon(\mathbf{k}+\mathbf{q})}. \tag{4.11}$$

It is crucial to take into account the effect of curvature of the dispersion in the noninteracting susceptibility $\chi_0^p$, i.e., the explicit form of $\varepsilon(\boldsymbol{k})$ given in Eq. (2.4) is retained in the calculation, to obtain a reasonable temperature dependence.

By using Eq. (4.10a) with the relations Eqs. (2.19) and (2.20), the uniform spin susceptibility $\chi_s(T)=\chi_{\rm uni}(q_\parallel,0,0)|_{q_\parallel\to 0}$ is calculated as

$$\chi_s(T)=\frac{\chi_0(T)}{1-g_{\sigma+}\chi_0(T)}, \tag{4.12}$$

where $\chi_0^+(0,0)=\chi_0^-(0,0)[\equiv\chi_0(T)/2]$. We note that the susceptibility $\chi_0(T)$ for $T=0$ is given by $\chi_0(0)=(v_{F,0}+v_{F,\pi})/(4\pi v_{F,0}v_{F,\pi})$, which reduces to $\chi_0(0)\to 1/(2\pi v_F)$ in the limit of a single chain because $v_{F,0},v_{F,\pi}\to v_F$.

All the diagrams given in Fig. 4 are nonsingular because only the small-$q_\parallel$ components are taken into account. The effect of the one-dimensional fluctuations appears through logarithmic corrections to $g_{\sigma+}$. This process can be accomplished by replacing the coupling constant $g_{\sigma+}$ with the renormalized one with the cutoff for finite temperature, i.e., $g_{\sigma+}(l=\ln\Lambda/T)$. Then the uniform spin susceptibility is given by

$$\chi_s(T)=\frac{\chi_0(T)}{1-g_{\sigma+}(l)\chi_0(T)}, \tag{4.13}$$

where $g_{\sigma+}(l)$ $[\equiv 2\pi v_F G_{\sigma+}(l)]$ is obtained by solving the RG equation Eq. (3.1b) or (3.12c). This formula is valid at the temperature above the energy scale of the gap $|m_t|$, since the coupling $g_{\sigma+}$ which describes the fluctuation of the Majorana triplet sector [see Eq. (3.3)] is treated perturbatively.

The overall temperature dependence of the uniform spin susceptibility is shown in Fig. 5. At sufficiently high temperature, the uniform susceptibility $\chi_s(T)$ exhibits behavior similar to the one-dimensional susceptibility both in the presence and in the absence of interactions. With decreasing temperature, $\chi_s(T)$ and $\chi_0(T)$ for the ladder system become larger than those of a single chain due to the enhancement of the density of states by interchain hopping. However, $\chi_s(T)$ shows activation behavior below $|m_t|$. In order to comprehend such low-temperature behavior, we estimate the spin susceptibility based on the effective theory for the spin mode, i.e., the Majorana-fermion theory. Below the energy scale of the gap $|m_t|$, we could ignore the fluctuation effects due to $g_{\sigma+}$ in Eq. (3.3), which would merely yield the mass renormalization given in Eq. (3.6a). Thus we can use the effective theory given by Eq. (3.7), although there remain some discussions on $g_{\sigma+}$.[59] By using Eq. (4.6) and after a straightforward calculation, we obtain the uniform susceptibility as

$$\chi_s(T)=\chi_{\rm uni}(q_\parallel,0,0)|_{q_\parallel\to 0}=\frac{1}{8\pi T}\int dk\,\mathrm{sech}^2\frac{\varepsilon_k^t}{2T}, \tag{4.14}$$

where $\varepsilon_k^t=(v_F^2k^2+m_t^2)^{1/2}$. For low $T$ $(\ll|m_t|)$, Eq. (4.14) is rewritten as

$$\chi_s(T)\approx\frac{1}{v_F}\sqrt{\frac{|m_t|}{2\pi T}}e^{-|m_t|/T}. \tag{4.15}$$

Thus we obtain the exponential decay of the spin susceptibility in the doped Hubbard ladder, which is the same low-temperature asymptotics as in the undoped Heisenberg ladder.[57,62]

The susceptibility at the QCP exhibits quite different behavior from that of $V=0$. Figure 6 shows the ladder $\chi_s(T)$ at low temperature for the doping near the QCP. Except for the QCP, the susceptibility exhibits activation behavior at low

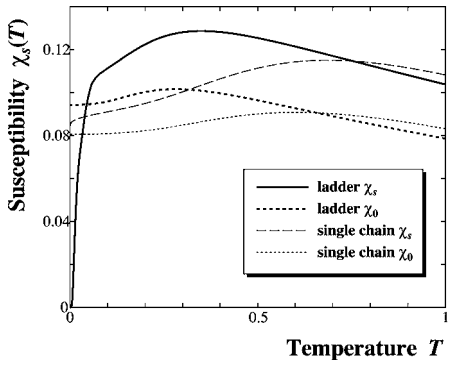


FIG. 5. The temperature dependence of several spin susceptibilities $\chi_s(T)$ and $\chi_0(T)$ for $U/t=4$, $V_\parallel=V_\perp=0$, and $\delta=0.1$, with $t_\parallel=t_\perp=1$, where $\chi_0$ denotes $\chi_s$ in the absence of interactions. The Majorana triplet gap is $m_t\approx 0.03$. For comparison, the corresponding susceptibilities of a single chain are also shown.

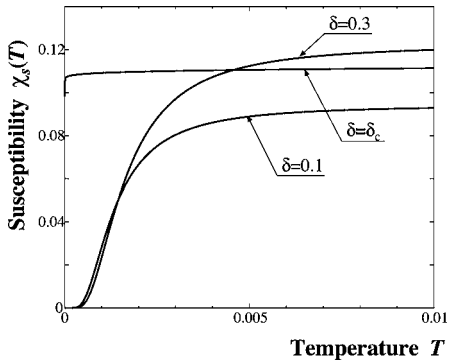


FIG. 6. The temperature dependence of the spin susceptibility for $U/t=3$, $V_{\parallel}=V_{\perp}=0.7$ with $t_{\parallel}=t_{\perp}=1$. The critical value of the doping is given by $\delta_c \approx 0.18$.

temperature. On the QCP, the susceptibility shows paramagnetic temperature dependence for the whole temperature region due to the absence of the gap $m_t$.

### B. NMR relaxation rate

In this section, we calculate the temperature dependence of the NMR relaxation rate $T_1^{-1}$. We use the general formula of the NMR relaxation rate[63]

$$T_1^{-1} = \frac{T}{2L}\sum_{\boldsymbol{q}} \frac{\chi''(\boldsymbol{q},\omega_0)}{\omega_0}, \tag{4.16}$$

where $\chi''$ is the imaginary part of the magnetic susceptibility and $\omega_0$ is the nuclear resonance frequency having a small energy of the order of millikelvins. Here we do not write the coefficient of the RHS of Eq. (4.16) by neglecting the momentum dependence of the hyperfine coupling constant, since the hyperfine coupling for the ladder-$^{63}$Cu site in $Sr_{14}Cu_{24}O_{41}$ originates mainly in the on-site hyperfine interaction and thus depends weakly on the momentum $\boldsymbol{q}$.[7] Since the interaction process between electrons near Fermi points is considered to play an important role for weak coupling, the integral over $q_{\parallel}$ in Eq. (4.16) can safely be split into two parts,

$$T_1^{-1} = (T_1^{-1})_{\mathrm{uni}} + (T_1^{-1})_{\mathrm{stag}}, \tag{4.17}$$

where $(T_1^{-1})_{\mathrm{uni}}$ and $(T_1^{-1})_{\mathrm{stag}}$ are the contributions from small $q_{\parallel}$ and large $q_{\parallel}$, respectively. Thus $(T_1^{-1})_{\mathrm{uni}}$ denotes the uniform contribution to the NMR relaxation rate, while $(T_1^{-1})_{\mathrm{stag}}$ is the antiferromagnetic staggered contribution. The explicit formulas are given by

$$(T_1^{-1})_{\mathrm{uni}} = \frac{T}{4\pi}\sum_{q_{\perp}} \int_{q_{\parallel}\approx 0} dq_{\parallel} \frac{\chi''_{\mathrm{uni}}(\boldsymbol{q},\omega_0)}{\omega_0}, \tag{4.18a}$$

$$(T_1^{-1})_{\mathrm{stag}} = \frac{T}{4\pi}\sum_{q_{\perp}} \int_{q_{\parallel}\approx \pm 2k_F} dq_{\parallel} \frac{\chi''(\boldsymbol{q},\omega_0)}{\omega_0}. \tag{4.18b}$$

These two contributions $(T_1^{-1})_{\mathrm{uni}}$ and $(T_1^{-1})_{\mathrm{stag}}$ show different temperature dependence. It has been discussed which contribution becomes dominant in Heisenberg ladder systems,[57,58,64,65] but the problem is still controversial. We treat these two contributions separately in the following.

#### 1. Uniform part: Contribution from small $q_{\parallel}$

Now we examine the uniform contribution $(T_1^{-1})_{\mathrm{uni}}$, by using the RPA calculation combined with the RG method at high temperature and by performing a direct calculation in terms of the low-energy effective theory at low temperature.

First we focus on the high-temperature behavior of $(T_1^{-1})_{\mathrm{uni}}$. In order to obtain $(T_1^{-1})_{\mathrm{uni}}$ from Eq. (4.18a), we calculate the imaginary part of the susceptibility $\chi''_{\mathrm{uni}}$. In the noninteracting case, one easily finds from Eq. (4.11) that the imaginary part of the noninteracting susceptibility becomes

$$\chi_0''(q_{\parallel},0,\omega) = \frac{1}{4}\sum_{p} pq_{\parallel}\delta(\omega - pv_F q_{\parallel}), \tag{4.19a}$$

$$\chi_0''(q_{\parallel},\pi,\omega) = \frac{1}{8}\sum_{p,\zeta} (pq_{\parallel} + 2\zeta\lambda)\delta(\omega - pv_F q_{\parallel} - 2\zeta v_F\lambda), \tag{4.19b}$$

where $\chi_0''(q_{\parallel},q_{\perp},\omega) \equiv \Sigma_{p=\pm}\mathrm{Im}\,\chi_0^p(q_{\parallel},q_{\perp},\omega)$ and we have neglected the curvature of the dispersion and used the linearized dispersion $\varepsilon(k_{\parallel},k_{\perp}) \to v_F(pk_{\parallel} - k_{F,k_{\perp}})$ in Eq. (4.11). Since $\chi_0''(\boldsymbol{q},\omega)$ is proportional to $\omega$ due to the $\delta$ function, the integral in Eq. (4.18a) is determined by the contribution being linear in $\chi_0''$ in $\chi_{\mathrm{uni}}(q_{\parallel},0,\omega)$ [Eq. (4.10a)]. Further, by neglecting the $q_{\parallel}$ and $\omega$ dependence of $\mathrm{Re}\,\chi_0^p(q_{\parallel},0,\omega)$ (which is a nonsingular quantity) in Eq. (4.10a), the imaginary part of $\chi_{\mathrm{uni}}(q_{\parallel},0,\omega)$ for small $q_{\parallel}$ and small $\omega$ is given by

$$\chi''_{\mathrm{uni}}(q_{\parallel},0,\omega) \approx \frac{\chi_0''(q_{\parallel},0,\omega)}{[1 - g_{\sigma+}\chi_0'(0,0,0)]^2} \approx \frac{1}{4}\frac{\chi_s^2(T)}{\chi_0^2(T)}\sum_{p} pq_{\parallel}\delta(\omega - pv_F q_{\parallel}), \tag{4.20}$$

where $\chi_0'(q_{\parallel},q_{\perp},\omega) \equiv \Sigma_{p=\pm}\mathrm{Re}\,\chi_0^p(q_{\parallel},q_{\perp},\omega)$ and $\chi_0(T) \equiv \chi'(0,0,0)$. In the second equality of Eq. (4.20), we have used Eqs. (4.13) and (4.19a). On the other hand, there is no correction to the $q_{\perp}=\pi$ component, i.e., $\chi''_{\mathrm{uni}}(q_{\parallel},\pi,\omega) = \chi_0''(q_{\parallel},\pi,\omega)$. By inserting Eqs. (4.20) and (4.19b) into Eq. (4.18a), the uniform contribution $(T_1^{-1})_{\mathrm{uni}}$ at $T \gg m_s, |m_t|$ is given by

$$(T_1^{-1})_{\mathrm{uni}} = \frac{T}{8\pi v_F^2}\frac{\chi_s^2(T)}{\chi_0^2(T)} + \frac{T}{8\pi v_F^2}. \tag{4.21}$$

The first (second) term in the RHS of Eq. (4.21) comes from processes with momentum transfer $q_{\perp}=0$ ($q_{\perp}=\pi$). The contribution with $q_{\perp}=\pi$, which takes the same form as in the noninteracting case, shows the Korringa law $T_1^{-1} \propto T$, while the contribution with $q_{\perp}=0$ is enhanced by the spin fluctuations yielding a factor $\chi_s^2(T)/\chi_0^2 = 1/[1 - g_{\sigma+}(T)\chi_0(T)]^2$. The contribution of $q_{\perp}=0$ shows a relation between the uniform part of the relaxation rate and the uniform spin susceptibility $\chi_s(T)$.

Next we calculate $(1/T_1)_{\mathrm{uni}}$ at low temperature by using the low-energy effective spin Hamiltonian (3.7), which is

valid at $T \ll m_{\rho-}$. By using Eqs. (3.7) and (4.6), we obtain

$$(T_1^{-1})_{\rm uni} = \frac{1}{16\pi v_F^2}\int_{|m_t|}^{\infty} d\varepsilon \frac{\varepsilon^2 + m_t^2}{\sqrt{(\varepsilon^2 - m_t^2)[(\varepsilon+\omega_0)^2 - m_t^2]}} \mathrm{sech}^2\frac{\varepsilon}{2T} + \frac{1}{16\pi v_F^2}\int_{\max(|m_t|,m_s)}^{\infty} d\varepsilon \frac{\varepsilon^2 + m_t m_s}{\sqrt{(\varepsilon^2 - m_t^2)(\varepsilon^2 - m_s^2)}} \mathrm{sech}^2\frac{\varepsilon}{2T}, \tag{4.22}$$

where $\varepsilon_k^z = (v_F^2 k^2 + m_z^2)^{1/2}$ with $z = t, s$ and we have set $\omega_0 \to 0$ in the second term of the RHS. The first term in the RHS of Eq. (4.22) is a contribution from the processes with momentum transfer $q_\perp = 0$, which is given by the Majorana triplet-triplet bubble in the diagram.[57] On the other hand, the second term is a contribution from processes with $q_\perp = \pi$ and corresponds to the Majorana triplet-singlet bubble. In the limit of high temperature, Eq. (4.22) reduces to $(T_1^{-1})_{\rm uni} = T/8\pi v_F^2 + T/8\pi v_F^2$ corresponding to the Korringa law. The enhancement factor in the first term of the RHS of Eq. (4.21) is not reproduced since the spin fluctuation has been neglected in Eq. (4.22). At low temperature ($\omega_0 \ll T \ll |m_t|$), the most dominant term reads

$$\begin{aligned}(T_1^{-1})_{\rm uni} &\approx \frac{1}{4\pi v_F^2}\int_{|m_t|}^{\infty} d\varepsilon \frac{(\varepsilon^2 + m_t^2)e^{-\varepsilon/T}}{\sqrt{(\varepsilon^2 - m_t^2)[(\varepsilon+\omega_0)^2 - m_t^2]}} \\ &\approx \frac{|m_t|}{4\pi v_F^2} e^{-|m_t|/T} K_0\left(\frac{\omega_0}{2T}\right) \\ &\approx \frac{|m_t|}{4\pi v_F^2} e^{-|m_t|/T}\left[\ln\left(\frac{4T}{\omega_0}\right) - \gamma\right],\end{aligned} \tag{4.23}$$

where $K_0(z)$ is the modified Bessel function and $\gamma$ is Euler's constant. Equation (4.23) is equal to the formula obtained in the undoped two-leg Heisenberg ladder[60,62] and in the spin-1 Haldane spin chain.[66]

The overall temperature dependence of $(T_1^{-1})_{\rm uni}$ can be obtained by the interpolation between Eqs. (4.21) and (4.22). We show the temperature dependence of $(T_1^{-1})_{\rm uni}$ in the CDW+PDW phase in Fig. 7. In the SC$d$ phase, $(T_1^{-1})_{\rm uni}$ shows behavior qualitatively similar to Fig. 7. The dashed curve represents the $q_\perp = 0$ contribution while the dotted curve represents the $q_\perp = \pi$ contribution. The $q_\perp = \pi$ contribution exhibits activation behavior at temperatures below $m_s$, while the $q_\perp = 0$ contribution shows $T$-linear dependence at temperatures above $|m_t|$. For $T \ll |m_t|$, the NMR relaxation rate $(T_1^{-1})_{\rm uni}$ is governed by the first term in Eq. (4.22) and exhibits an activation behavior given by Eq. (4.23). The component with $q_\perp = 0$ is always larger than that with $q_\perp = \pi$ in the whole temperature region, in contrast to the results in Ref. 57. It is found that the total $(T_1^{-1})_{\rm uni}$ clearly exhibits behavior consisting of two components and thus the result cannot be fitted by a single activation energy.

#### 2. Staggered part: Contribution from large $q_\parallel$

We calculate the antiferromagnetic contribution $(T_1^{-1})_{\rm stag}$ given by Eq. (4.18b). As is known in the single-chain case,[55] both the spin and charge degrees of freedom contribute to

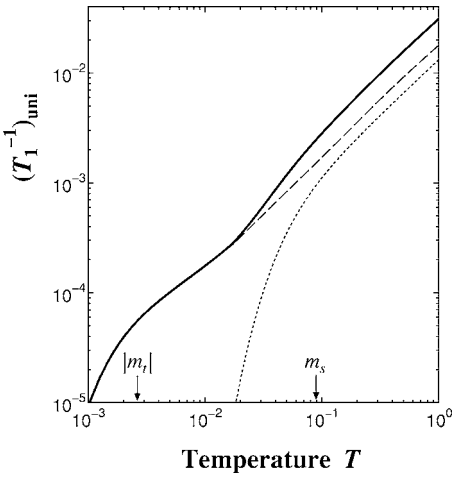


FIG. 7. The temperature dependence of the uniform contribution of the NMR relaxation rate, with $U/t=3$, $V_\parallel/t = V_\perp/t = 0.7$, $t \equiv t_\parallel = t_\perp = 1$, and $\delta = 0.1$. The dashed and dotted curves denote the $q_\perp = 0$ and $\pi$ contributions, respectively, and the solid curve denotes the total $(T_1^{-1})_{\rm uni}$.

$(T_1^{-1})_{\rm stag}$. The critical charge mode in our theory is the total sector $\phi_{\rho+}$, whose Hamiltonian is given by

$$\mathcal{H}_{\rho+} = \frac{v_{\rho+}}{2\pi}\left[\frac{1}{K_{\rho+}}(\partial_x \phi_{\rho+})^2 + K_{\rho+}(\partial_x \theta_{\rho+})^2\right], \tag{4.24}$$

where $v_{\rho+} = v_F[1 - (g_{\rho+}/2\pi v_F)^2]^{1/2}$ and $K_{\rho+} = [(2\pi v_F - g_{\rho+})/(2\pi v_F + g_{\rho+})]^{1/2} \approx 1 - G_{\rho+}$. For simplicity, we will neglect the normalization of the velocity and set $v_{\rho+} \to v_F$.

First we study $(T_1^{-1})_{\rm stag}$ at high temperature, i.e., $T \gg m_{\rho-}$. For the noninteracting case, the real part $\chi_0'$ becomes logarithmic singular, i.e., $\chi_0'(2k_F + q_\parallel, \pi, \omega, T) \approx (4\pi v_F)^{-1} \ln(\Lambda/x)$ where $x = \max(|v_F q_\parallel|, |\omega|, T)$, while the imaginary part $\chi_0''$ is nonsingular. The imaginary part of $\chi_0$ for $|\omega| \ll T$ is given by

$$\chi_0''(2k_F + q_\parallel, \pi, \omega, T) \approx \frac{\omega}{32 v_F T}\mathrm{sech}^2\left(\frac{v_F q_\parallel}{4T}\right). \tag{4.25}$$

By using the fact $|\chi_0'| \gg |\chi_0''|$, the imaginary part of $\chi$ is given by[55]

$$\chi''(2k_F + q_\parallel, \pi, \omega, T) = \bar{\chi}_{\rm stag}(q_\parallel, \omega, T)\chi_0''(2k_F + q_\parallel, \pi, \omega, T), \tag{4.26}$$

where $\bar{\chi}$ is an auxiliary function associated with the real part of $\chi$:

$$\bar{\chi}_{\rm stag}(q_\parallel, \omega, T) \equiv 4\pi v_F \frac{\partial\, \mathrm{Re}\, \chi(2k_F + q_\parallel, \pi, \omega, T)}{\partial \ln(\Lambda/x)}, \tag{4.27}$$

with $x = \max(|\omega|, |v_F q_\parallel|, T)$. The staggered part of the NMR relaxation rate can be obtained by inserting Eq. (4.26) into Eq. (4.18b). Since $\chi_0''(2k_F + q_\parallel, \pi, \omega, T)$ has a sharp peak around $q_\parallel = 0$ with the exponential decay for large $q_\parallel$, we rewrite $\bar{\chi}_{\rm stag}(q_\parallel, \omega, T)$ as $\bar{\chi}_{\rm stag}(T)$ in Eq. (4.26) by neglecting the $q_\parallel$ and $\omega$ dependence in $\bar{\chi}_{\rm stag}(q_\parallel, \omega, T)$. Then the staggered part $(T_1^{-1})_{\rm stag}$ is given by

$$(T_1^{-1})_{\rm stag} = \frac{T}{8\pi v_F^2}\bar{\chi}_{\rm stag}(T). \tag{4.28}$$

In order to examine $\bar{\chi}_{\rm stag}(T)$, we calculate the correlation function for $\boldsymbol{n}_-(x)$ [Eq. (4.4)] which denotes the spin operator with momentum transfer $q_\parallel \approx 2k_F$ and $q_\perp = \pi$. By applying the RG method to the spin-spin correlation function $R(x,\tau) = \langle T_\tau n_-^\alpha(x,\tau) n_-^\alpha(0,0)\rangle$, the RG equation for $\bar{\chi}_{\rm stag}$ is obtained as

$$\frac{d}{dl}\ln \bar{\chi}_{\rm stag}(l) = \frac{1}{2}G_{\rho+} - \frac{1}{2}G_{\rho-} + \frac{1}{2}G_{\sigma+} - \frac{1}{2}G_{\sigma-} + \frac{1}{2}G_{\bar{c}-,st} + \frac{1}{2}G_{\bar{c}-,ss} \tag{4.29}$$

where $l = \ln(\Lambda/T)$ and $\bar{\chi}_{\rm stag}(0) = 1$. To obtain the temperature dependence of $(T_1^{-1})_{\rm stag}$ from Eq. (4.28), we first solve the RG equations (3.1) for the coupling constants, and next substitute those into Eq. (4.29). We note that, for the noninteracting case, the auxiliary function is given by $\bar{\chi}_{\rm stag}(l) = 1$ and then $(T_1^{-1})_{\rm stag} = T/8\pi v_F^2$, which has the same temperature dependence as the uniform part [Eq. (4.21)] in the noninteracting limit.

At temperature below the charge gap $m_{\rho-}$, i.e., for $l > l_{\rho-}$, the field $\theta_{\rho-}$ can be replaced by its average value $\langle\theta_{\rho-}\rangle$. Without losing generality, we can assume that $\theta_{\rho-}$ is locked at $\langle\theta_{\rho-}\rangle = \pi I$ where $I$ is integer. Then the spin operators are given by

$$n_-^x(x) \propto \cos\tilde{\phi}_{\rho+} \sin\theta_{\sigma+} \cos\phi_{\sigma-}, \tag{4.30a}$$

$$n_-^y(x) \propto \cos\tilde{\phi}_{\rho+} \cos\theta_{\sigma+} \cos\phi_{\sigma-}, \tag{4.30b}$$

$$n_-^z(x) \propto \cos\tilde{\phi}_{\rho+} \cos\phi_{\sigma+} \sin\theta_{\sigma-}, \tag{4.30c}$$

where $\tilde{\phi}_{\rho+}$ is defined just after Eq. (4.8). The RG equation for $\bar{\chi}_{\rm stag}(T)$ is given by

$$\frac{d}{dl}\ln \bar{\chi}_{\rm stag}(l) = \frac{1}{2} + \frac{1}{2}G_{\rho+} + \frac{1}{2}G_{\sigma+} - \frac{1}{2}G_{\sigma-} + M_t + M_s, \tag{4.31}$$

where the coupling constants are calculated from Eq. (3.12). Thus the NMR relaxation rate $(T_1^{-1})_{\rm stag}$ in the region of $\max(|m_t|, m_s) \ll T \ll m_{\rho-}$ is given by Eqs. (4.28) and (4.31). However, in the present system, we find $m_s \approx m_{\rho-}$, and then this asymptotic behavior would not be realized.

Next we calculate the antiferromagnetic contribution to the relaxation rate at low temperature by using the effective spin Hamiltonian (3.7). In this case, the staggered components of the spin operators (4.30) are rewritten as

$$n_-^x(x) \approx \cos\tilde{\phi}_{\rho+}(\sigma_1\mu_2\mu_3)\mu_4, \tag{4.32a}$$

$$n_-^y(x) \approx \cos\tilde{\phi}_{\rho+}(\mu_1\sigma_2\mu_3)\mu_4, \tag{4.32b}$$

$$n_-^z(x) \approx \cos\tilde{\phi}_{\rho+}(\mu_1\mu_2\sigma_3)\mu_4, \tag{4.32c}$$

where the Klein factors have been omitted. We follow the calculation performed in Refs. 58, 67, and 68. If the spin-spin correlation function at zero temperature exhibits power-law behavior with exponent $\eta$, i.e., $\langle n_-(x)n_-(0)\rangle \propto x^{-\eta}$, it can be shown that the temperature dependence of the NMR relaxation rate is given by $(T_1^{-1})_{\rm stag} \propto T^{\eta-1}$, by using the conformal mapping technique.[68] If $|m_t|, |m_s| \ll T \ll m_{\rho-}$ is realized, the exponent is $\eta = \frac{1}{2}K_{\rho+} + 1$ and then we obtain

$$(T_1^{-1})_{\rm stag} \propto T^{K_{\rho+}/2}. \tag{4.33}$$

This behavior, however, would not be observed since $m_s \approx m_{\rho-}$. For $|m_t| \ll T \ll |m_s|$ in the SC$d$ or CDW+PDW phase, we can replace $\mu_4$ by its average value $\langle\mu_4\rangle \neq 0$ in Eq. (4.32) and then the exponent of the spin-spin correlation function becomes $\eta = \frac{1}{2}K_{\rho+} + \frac{3}{4}$. Thus we have

$$(T_1^{-1})_{\rm stag} \propto T^{-1/4+K_{\rho+}/2}. \tag{4.34}$$

In the limit of low temperature ($T \ll |m_t|, |m_s|, m_{\rho-}$), the relaxation rate exhibits thermally activated behavior. In the SC$d$ phase ($m_t > 0$), we obtain (see the Appendix)

$$(T_1^{-1})_{\rm stag} \propto \sum_{\epsilon=\pm}\int_{-\infty}^{\infty}\frac{d\omega}{2\pi}\cosh\left(i\epsilon\frac{\pi}{2}\eta + \frac{\omega}{2T}\right)\left(\frac{2\pi T}{v_F}\right)^{\eta-1} B\left(\frac{\eta}{2} - i\epsilon\frac{\omega}{2\pi T}, 1-\eta\right) \times \int_{-\infty}^{\infty}\frac{d\theta_1}{2\pi}\frac{d\theta_2}{2\pi}\frac{d\theta_3}{2\pi}\frac{2\pi\delta(E(\theta_1) - E(\theta_2) + E(\theta_3) + \omega)}{8\cosh[E(\theta_1)/2T]\cosh[E(\theta_2)/2T]\cosh[E(\theta_3)/2T]}\coth^2\left(\frac{\theta_1-\theta_2}{2}\right), \tag{4.35}$$

where $E(\theta) = |m_t|\cosh\theta$ is the rapidity representation of dispersion, $B(x,y)$ is the beta function, and $\eta = K_{\rho+}/2$. In the low-temperature limit $T \ll m_t$, the staggered part of the NMR relaxation rate in the SC$d$ state is given by (see the Appendix)

$$(T_1^{-1})_{\rm stag} \propto T^{1+K_{\rho+}/2}\exp(-2m_t/T), \tag{4.36}$$

showing the activation behavior with a gap $2m_t$. On the other hand, in the CDW+PDW state ($m_t < 0$), by considering two

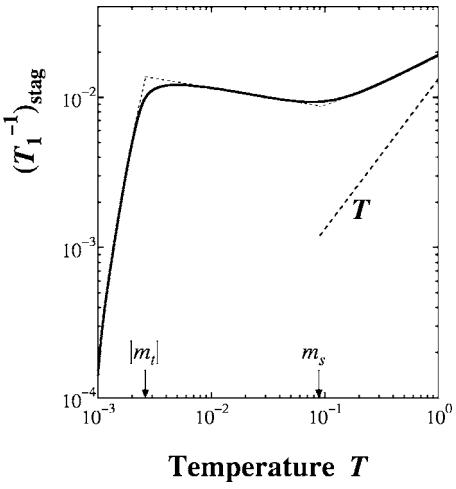


FIG. 8. The temperature dependence of the NMR relaxation rate $(T_1^{-1})_{\text{stag}}$ for $U/t=3$, $V_{\parallel}/t=V_{\perp}/t=0.7$, $t\equiv t_{\parallel}=t_{\perp}=1$, and $\delta=0.1$.

magnon process, the NMR relaxation rate would be given by (see the Appendix)

$$(T_1^{-1})_{\text{stag}} \propto T^{K_{\rho+}/2}\exp(-|m_t|/T)\ln T. \tag{4.37}$$

In Fig. 8, we show the staggered part of the NMR relaxation rate, $(T_1^{-1})_{\text{stag}}$ at low temperature, which is calculated based on Eqs. (4.33), (4.34), and (4.36). The enhancement of $(T_1^{-1})_{\text{stag}}$ in the interval region of $|m_t|<T<m_s$, which is similar to that of single chain, originates in the antiferromagnetic fluctuations. The rapid decrease of $(T_1^{-1})_{\text{stag}}$ at temperature of $T<|m_t|$ shares the common feature with $(T_1^{-1})_{\text{uni}}$ and $\chi_s$. We note that the relative magnitude of $(T_1^{-1})_{\text{uni}}$ and $(T_1^{-1})_{\text{stag}}$ depends on those of their hyperfine couplings.

### C. Quantum critical behavior

Finally we focus on the temperature dependence of $\chi_s$, $(T_1^{-1})_{\text{uni}}$, and $(T_1^{-1})_{\text{stag}}$, just above the QCP, i.e., $m_t=0$. Since the $g_{\sigma+}$ term becomes marginally irrelevant in the effective theory (3.3), we first examine the scaling of $g_{\sigma+}$, which gives rise to logarithmic corrections for the physical quantities.

In the effective spin Hamiltonian (3.3), we consider the temperature region lower than the gap in the Majorana singlet sector. In this case, we can integrate out the $\xi^4$ degrees of freedom and then we can rewrite $m_t^0 - ig_{\sigma-}\langle\xi_+^4\xi_-^4\rangle \to m_t^0$. Further we can set $m_t^0=0$ on the critical point. Then only the $g_{\sigma+}$ term remains where the RG equation is given by

$$\frac{d}{dl}G_{\sigma+}(l) = -G_{\sigma+}^2(l), \tag{4.38}$$

and $g_{\sigma+}(l)=(2\pi v_F)G_{\sigma+}(l)$. By solving Eq. (4.38), we have

$$g_{\sigma+}(l) = \frac{g_{\sigma+}}{1+(g_{\sigma+}/2\pi v_F)(l-l_s)}, \tag{4.39}$$

where the initial value is given by $g_{\sigma+}(l_s)=g_{\sigma+} \equiv (2\pi v_F)G_{\sigma+}(l_s)$. The quantity $l_s$ corresponds to the scale of the gap in the Majorana singlet excitation, $m_s \approx \Lambda e^{-l_s}$.

From Eq. (4.38), the character of the phase transition is determined by the sign of the initial value of $G_{\sigma+}$.[31,33,51] When the initial value is given by $G_{\sigma+}(l_s)>0$, the coupling constant $G_{\sigma+}(l)$ decreases to zero under renormalization, and then becomes marginally irrelevant. In this case, the effective theory in the low-temperature limit leads to the *noninteracting* massless Majorana fermion, and thus the system exhibits a quantum critical behavior. On the other hand, for the initial value being negative, i.e., $G_{\sigma+}(l_s)<0$, the coupling constant $G_{\sigma+}(l)$ becomes marginally relevant due to its divergence at $l_t=2\pi v_F/|g_{\sigma+}|$. In this case, the effective theory does not give a quantum critical behavior due to a mass gap $m_t \approx \Lambda e^{-2\pi v_F/|g_{\sigma+}|}$, even if the bare mass $m_t^0$ reduces to zero. From the numerical calculation of Eqs. (3.1) and (3.12), we have confirmed that the coupling constant $G_{\sigma+}$ at $l=l_s$ is positive within our choice of repulsive interactions, and that the present ladder system corresponds to the former case, i.e., the system exhibits the quantum critical behavior. If the sign of $G_{\sigma+}(l_t)$ could be changed by another type of interaction in the microscopic Hamiltonian,[31,33] the first-order transition would be obtained instead of the QCP within the present framework.

In the following we examine the temperature dependence of $\chi_s(T)$, $(T_1^{-1})_{\text{uni}}$, and $(T_1^{-1})_{\text{stag}}$, separately by using Eq. (4.39) with $l=\ln(\Lambda/T)$ where $\Lambda$ is a high-energy cutoff of the order of the bandwidth. We note that at low temperature, i.e., for large $l$, the renormalized coupling constant shows $g_{\sigma+}(l) \approx 2\pi v_F/\ln(\Lambda/T)$.

#### 1. The uniform spin susceptibility $\chi_s(T)$

We can use the formula (4.13) for calculating the uniform spin susceptibility since $m_t=0$ at the QCP. By inserting Eq. (4.39) into Eq. (4.13), the temperature dependence of $\chi_s(T)$ is obtained with the low-temperature asymptotics,

$$\chi_s(T) \approx \frac{1}{2\pi v_F}\left[1+\frac{1}{\ln(\Lambda/T)}\right]. \tag{4.40}$$

Figure 6 shows the temperature dependence of $\chi_s(T)$ where $\delta=\delta_c$ corresponds to the QCP. Equation (4.40) is compared with the spin susceptibility for the $S=\frac{1}{2}$ Heisenberg single chain given by[69]

$$\chi_s^{\text{1D}}(T) \approx \frac{1}{2\pi v}\left[1+\frac{1}{2}\frac{1}{\ln(\Lambda/T)}\right], \tag{4.41}$$

where $v=\pi J/2$ and $J$ is the exchange interaction. The results (4.40) and (4.41) are consistent with the susceptibility in the $SU(2)_k$ WZNW critical theory with marginally irrelevant operators, which gives the logarithmic correction $\{1+k/[2\ln(\Lambda/T)]\}$ where $k$ is the level of SU(2) algebra.[70] Note that $k=2$ for a two-leg ladder, while $k=1$ for the $S=\frac{1}{2}$ single chain.

#### 2. The NMR relaxation rate: $(T_1^{-1})_{uni}$ and $(T_1^{-1})_{stag}$

The temperature dependence of $(T_1^{-1})_{\text{uni}}$ can be obtained by inserting Eq. (4.40) into Eq. (4.21). The second term of the RHS of Eq. (4.21) can be discarded since this would show the exponential decay at temperature below $m_s$ as seen from the dotted curve of Fig. 9. For the low-temperature limit, we have

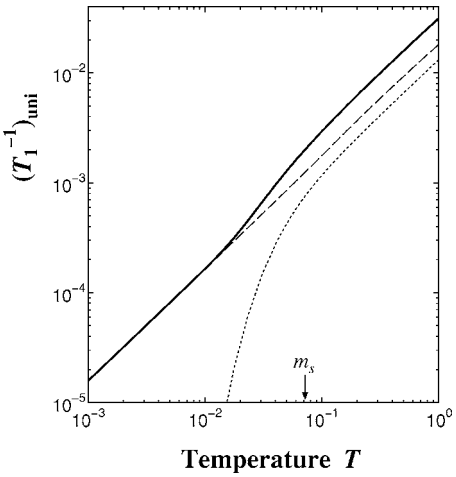


FIG. 9. The temperature dependence of the NMR relaxation rate with $U/t=3$, $V_\parallel/t=V_\perp/t=0.7$, $t\equiv t_\parallel=t_\perp=1$, and $\delta=\delta_c\approx 0.18$. The power-law behavior is retained even in the limit of low temperature due to the vanishing of the Majorana triplet mass, i.e., $m_t=0$. The dashed and dotted curves correspond to the contributions with $q_\perp=0$ and $\pi$, respectively, while the solid curve denotes the total $(T_1^{-1})_{\rm uni}$.

$$(T_1^{-1})_{\rm uni} \approx \frac{T}{8\pi v_F^2}\left[1+\frac{2}{\ln(\Lambda/T)}\right]. \tag{4.42}$$

The overall temperature dependence of $(T_1^{-1})_{\rm uni}$ at the QCP is shown in Fig. 9. For the single chain with $S=\frac{1}{2}$, we have

$$(T_1^{-1})_{\rm uni}^{\rm 1D} \approx \frac{T}{4\pi v_F^2}\frac{[\chi_s^{\rm 1D}(T)]^2}{\chi_0^2(T)} \approx \frac{T}{4\pi v_F^2}\left[1+\frac{1}{\ln(\Lambda/T)}\right], \tag{4.43}$$

where the first equality is obtained in Ref. 55.

The logarithmic correction to the staggered part $(T_1^{-1})_{\rm stag}$ can be obtained as follows. If one neglects the marginally irrelevant $g_{\sigma+}$, the staggered part $(T_1^{-1})_{\rm stag}$ is given by Eq. (4.34). In order to retain the renormalization effect of $g_{\sigma+}$, we use Eq. (4.28). In a way similar to the derivation of Eq. (4.38), the scaling equation of the auxiliary field $\bar{\chi}_{\rm stag}(T)$ on the QCP at temperature below $m_s$ is given by

$$\frac{d}{dl}\ln\bar{\chi}_{\rm stag}(l) = \frac{3}{4}+\frac{1}{2}G_{\rho+}+\frac{1}{2}G_{\sigma+}(l), \tag{4.44}$$

where $G_{\rho+}$ is independent of $l$ and the factor 3/4 in the RHS is determined from the scaling dimension of the spin operator Eq. (4.32), i.e., $(2-2\,\dim[\cos\tilde{\phi}_{\rho+}]-2\,\dim[\sigma_1\mu_2\mu_3])=3/4$. By solving Eq. (4.44) with $K_\rho=1-G_{\rho+}$, we have

$$\bar{\chi}_{\rm stag}(T) = \left(\frac{T}{\Lambda}\right)^{-5/4+K_{\rho+}/2}\sqrt{1+\frac{g_{\sigma+}}{2\pi v_F}\ln\left(\frac{\Lambda}{T}\right)}. \tag{4.45}$$

From Eqs. (4.28) and (4.45), we obtain the low-temperature asymptotics of $(T_1^{-1})_{\rm stag}$ as

$$(T_1^{-1})_{\rm stag} \propto T^{-1/4+K_{\rho+}/2}\sqrt{\ln\left(\frac{\Lambda}{T}\right)}. \tag{4.46}$$

This result is compared with the staggered component of $T_1^{-1}$ for the single chain, which is given by

$$(T_1^{-1})_{\rm stag}^{\rm 1D} \propto T^{K_\rho}\sqrt{\ln\left(\frac{\Lambda}{T}\right)}. \tag{4.47}$$

We note that, in the insulating state ($K_\rho\to 0$), Eq. (4.47) is reduced to $(T_1^{-1})_{\rm stag}^{\rm 1D}\to\sqrt{\ln(\Lambda/T)}$ reproducing the result of the $S=\frac{1}{2}$ Heisenberg spin chain,[71] while Eq. (4.46) leads to $(T_1^{-1})_{\rm stag}\to T^{-1/4}\sqrt{\ln(\Lambda/T)}$, which is consistent with the result obtained in Ref. 58 except for the logarithmic correction.

## V. CONCLUSIONS AND DISCUSSION

In the present paper, we have examined the ground-state phase diagram and the temperature dependence of the susceptibility and the NMR relaxation rate for the extended two-leg Hubbard model away from half filling, by using the weak-coupling bosonization method. In the ground state, we have clarified the competition between the SC$d$ state and the CDW+PDW state and have shown the quantum critical behavior close to the transition point where the SC$d$ state changes into the CDW+PDW state with increasing the nearest-neighbor repulsion and/or decreasing doping rate. At finite temperature, the magnetic response exhibits characteristic property coming from two modes of spin excitations. Especially on the quantum critical point, we found that the spin susceptibility shows paramagnetic temperature dependence with logarithmic corrections and the NMR relaxation rate exhibits anomalous power-law behavior.

Here we discuss the commensurability effect due to the umklapp scattering, which would play an important role close to half filling. At half filling, the umklapp scattering is given by[33]

$$\begin{aligned}\mathcal{H}_{\rm umklapp} = \frac{1}{4}\sum_{p,\sigma}\sum_{\zeta_i=\pm}{}'\big[&g_{3\parallel}^{\epsilon\bar{\epsilon}}\psi_{p,\sigma,\zeta_1}^\dagger\psi_{p,\sigma,\zeta_2}^\dagger\psi_{-p,\sigma,\zeta_4}\psi_{-p,\sigma,\zeta_3}\\ &+ g_{3\perp}^{\epsilon\bar{\epsilon}}\psi_{p,\sigma,\zeta_1}^\dagger\psi_{p,-\sigma,\zeta_2}^\dagger\psi_{-p,-\sigma,\zeta_4}\psi_{-p,\sigma,\zeta_3}\big],\end{aligned} \tag{5.1}$$

where $g_{3\parallel}^{\epsilon\bar{\epsilon}}=l_\epsilon V_\perp+m_{3,\epsilon}V_\parallel$ and $g_{3\perp}^{\epsilon\bar{\epsilon}}=(U+l_\epsilon V_\perp+m_{3,\epsilon}V_\parallel)$ with the numerical factors $l_\pm=\pm 1$, $m_{3,+}=-1$, and $m_{3,-}=-2$. In terms of bosonic fields, Eq. (5.1) is rewritten as

$$\begin{aligned}\mathcal{H}_{\rm umklapp} = \frac{1}{2\pi^2a^2}\big[&g_{c+,\bar{c}-}\cos 2\phi_{\rho+}\cos 2\theta_{\rho-}\\ &+ g_{c+,s+}\cos 2\phi_{\rho+}\cos 2\phi_{\sigma+}\\ &+ g_{c+,s-}\cos 2\phi_{\rho+}\cos 2\phi_{\sigma-}\\ &+ g_{c+,\bar{s}-}\cos 2\phi_{\rho+}\cos 2\theta_{\sigma-}\big],\end{aligned} \tag{5.2}$$

where the coupling constant are $g_{c+,\bar{c}-}=-g_{3\perp}^{-+}$, $g_{c+,s+}=-g_{3\parallel}^{+-}+g_{3\parallel}^{--}$, $g_{c+,s-}=-g_{3\perp}^{+-}$, and $g_{c+,\bar{s}-}=+g_{3\perp}^{--}$. For the rung-singlet state at half filling, the renormalized coupling constants in Eq. (5.2) are given by $g_{c+,\bar{c}-}^*<0$, $g_{c+,s+}^*<0$, $g_{c+,s-}^*<0$, and $g_{c+,\bar{s}-}^*=0$. Even in the presence of a few holes, the renormal-

ized umklapp scattering would remain finite unless at extremely low energy scale. Then here we fix the amplitude of the umklapp scattering and discuss the effect of the finite doping. In terms of phase variable, the particle number operator is given by

$$N = \sum_{j,l,\sigma} \left( c^{\dagger}_{j,l,\sigma} c_{j,l,\sigma} - \frac{1}{2} \right) = \frac{2}{\pi} [\phi_{\rho+}(\infty) - \phi_{\rho+}(-\infty)]. \tag{5.3}$$

From Eq. (5.3), the injection of a single electron or hole corresponds to the formation of the $\pi/2$ soliton or antisoliton in the $\phi_{\rho+}$ mode. In order to avoid the increase of energy, the $\pi/2$ soliton in the $\phi_{\rho+}$ mode is always accompanied by the $\pi/2$ solitons in the $\phi_{\sigma+}$, $\theta_{\rho-}$, and $\phi_{\sigma-}$ modes. This fact implies that the $\pi/2$ soliton in the $\phi_{\rho+}$ mode involves the appearance of local spin at the same rung. On the other hand, the $\pi$ soliton in the $\phi_{\rho+}$ mode, which corresponds to $N=2$, is not accompanied by solitons in the spin and other modes. Thus, if a $\pi/2$ soliton in the $\phi_{\rho+}$ mode is created in the system, the free spin appears at the same rung in the bulk rung-singlet state and the spin-charge separation does not take place. This picture would connect with the strong-coupling one in the sense that holes can destroy spin singlets in the two-leg ladder systems.[2]

Finally we compare the present results with the experimental ones on the two-leg ladder compounds $Sr_{14-x}Ca_xCu_{24}O_{41}$, which have the characteristic features of the spin-gapped normal state and the superconducting state. For $x=12$ and under a pressure of 3.5 GPa, the NMR measurements show two excitation modes above the SC state, where $T_1^{-1}$ decreases rapidly at higher temperature and $T$-linear dependence is found at lower temperature.[12] This result resembles the present result of Figs. 7 and 9. The decrease for $T > m_s$ comes from the formation of the spin gap in the spin-singlet excitations while the linear dependence for $|m_t| < T < m_s$ appears due to the gapless mode with the freedom of spin-triplet excitations. Such an interval region is enlarged close to the QCP since $m_t \to 0$ at the QCP, as seen from Fig. 3. From the NMR shifts, it is shown that the uniform magnetic susceptibility decreases slowly for $30 < T < 200$ K and stays constant for $T < 30$ K. The former resembles Fig. 5 where the slow decrease below $T/t < 0.3$ is due to the band effect. The latter would correspond to Fig. 6 with $\delta=0.1$, where $\chi_s$ is almost independent of temperature for $0.07 < T/t < 0.01$. Thus the present scenario of two spin excitations could be relevant to experiments although the present approach is based on weak-coupling theory.

## ACKNOWLEDGMENTS

M.T. thanks A. Furusaki, E. Orignac, and O. A. Starykh for valuable discussions. This work was supported by a Grant-in-Aid for Scientific Research on Priority Areas of Molecular Conductors (Grant No. 15073213) from the Ministry of Education, Culture, Sports, Science and Technology, Japan.

## APPENDIX: STAGGERED PART OF THE NMR RELAXATION RATE IN THE LOW-TEMPERATURE LIMIT

In this appendix, we derive the staggered part of the NMR relaxation rate $(T_1^{-1})_{\rm stag}$ in the low-temperature limit [Eqs. (4.35)–(4.37)], based on the Majorana-fermion description of the effective theory.

In the temperature region $T \ll (|m_s|, m_{\rho-})$, the staggered component of the spin operator [Eq. (4.32)] is rewritten as

$$n^x_- \propto \cos \tilde{\phi}_{\rho+}(\sigma_1 \mu_2 \mu_3), \tag{A1a}$$

$$n^y_- \propto \cos \tilde{\phi}_{\rho+}(\mu_1 \sigma_2 \mu_3), \tag{A1b}$$

$$n^z_- \propto \cos \tilde{\phi}_{\rho+}(\mu_1 \mu_2 \sigma_3), \tag{A1c}$$

where $\tilde{\phi}_{\rho+} = \phi_{\rho+} - \pi \delta x$. In terms of these operators, the NMR relaxation rate is given by

$$(T_1^{-1})_{\rm stag} \propto \int_{-\infty}^{\infty} dt\, S(t), \tag{A2}$$

where $S(t) = \langle n^{\alpha}_-(x=0,t) n^{\alpha}_-(0,0) \rangle$ is the local correlation function at finite temperature. We will estimate this correlation function by using the effective Hamiltonian (3.8) and (4.24). Since the charge and spin degrees of freedom are decoupled, the correlation function can be rewritten as

$$S(t) = S_{\rho+}(t) S_{\rm Ising}(t), \tag{A3}$$

where

$$S_{\rho+}(t) \equiv \langle \cos \phi_{\rho+}(0,t) \cos \phi_{\rho+}(0,0) \rangle, \tag{A4a}$$

$$S_{\rm Ising}(t) \equiv \langle \mu(0,t) \mu(0,0) \rangle^2 \langle \sigma(0,t) \sigma(0,0) \rangle. \tag{A4b}$$

One can easily find that all the correlation functions $\langle n^{\alpha}_-(0,t) n^{\alpha}_-(0,0) \rangle$ for $\alpha = x,y,z$ become identical, since the system has spin-rotational symmetry.

The local correlation function for the charge fields is given by[67]

$$\begin{aligned} S_{\rho+}(t) &= \frac{1}{2} e^{-i(\pi/2)\eta\, \mathrm{sgn}(t)} \left[ \frac{\pi T a/v}{\sinh(\pi T |t|)} \right]^{\eta} \\ &= \int_{-\infty}^{\infty} \frac{d\omega}{2\pi} e^{-i\omega t} \sum_{\epsilon=\pm} \frac{a}{2v} e^{-i(\pi/2)\eta} \left( \frac{2\pi T a}{v} \right)^{\eta-1} \\ &\quad \times B\left( \frac{\eta}{2} - i\epsilon \frac{\omega}{2\pi T}, 1-\eta \right), \end{aligned} \tag{A5}$$

where $\eta = K_{\rho+}/2$ and $B(x,y)$ is the beta function $B(x,y) = \Gamma(x)\Gamma(y)/\Gamma(x+y)$. In the second equality, we have performed the Fourier transformation.[67]

The correlation function for the Ising fields at finite temperature can be calculated following Ref. 72. The asymptotic behavior of the Ising correlation function depends on whether the system is in the ordered phase or in the disordered phase, i.e., depends on the sign of the mass $m_t$.

In the SC$d$ phase ($m_t > 0$), the Ising systems $\sigma_i$ ($i=1, 2, 3$) are in the disordered phase; thus $\mu_i$ has a nonzero expecta-

tion value. In this case, the dominant contribution in the low-temperature limit is[58]

$$S_{\rm Ising}(t)\Big|_{m_t>0} \propto \sum_{\epsilon,\epsilon_3=\pm}\int_{-\infty}^{\infty}\frac{d\theta_1}{2\pi}\frac{d\theta_2}{2\pi}\frac{d\theta_3}{2\pi} \times f_{\epsilon}(\theta_1)f_{-\epsilon}(\theta_2)f_{\epsilon_3}(\theta_3)\coth^2\left(\frac{\theta_1-\theta_2}{2}\right) \times e^{-i[\epsilon E(\theta_1)-\epsilon E(\theta_2)+\epsilon_3 E(\theta_3)]t}, \quad \text{(A6)}$$

where $E(\theta)=|m_t|\cosh\theta$ and $f_{\epsilon}(\theta)=[1+e^{-\epsilon E(\theta)/T}]^{-1}$. By inserting Eqs. (A5) and (A6) into Eq. (A3), and inserting it into Eq. (A2), we obtain Eq. (4.35).

In the CDW+PDW phase ($m_t<0$), the Ising systems are now in the ordered phase; thus $\sigma_i$ has a nonzero expectation value. In this case the dominant contribution at low temperature reads

$$S_{\rm Ising}(t)\Big|_{m_t<0} \propto \sum_{\epsilon=\pm}\int_{-\infty}^{\infty}\frac{d\theta_1}{2\pi}\frac{d\theta_2}{2\pi} \times f_{\epsilon}(\theta_1)f_{-\epsilon}(\theta_2)e^{-i\epsilon[E(\theta_1)-E(\theta_2)]t}. \quad \text{(A7)}$$

Then the NMR relaxation rate for $m_t<0$ is given by

$$(T_1^{-1})_{\rm stag} \propto \sum_{\epsilon=\pm}\int_{-\infty}^{\infty}\frac{d\omega}{2\pi}\cosh\left(i\epsilon\frac{\pi}{2}\eta+\frac{\omega}{2T}\right) \times\left(\frac{2\pi T}{v_F}\right)^{\eta-1}B\left(\frac{\eta}{2}-i\epsilon\frac{\omega}{2\pi T},1-\eta\right) \times\int_{-\infty}^{\infty}\frac{d\theta_1}{2\pi}\frac{d\theta_2}{2\pi}\frac{2\pi\delta(E(\theta_1)-E(\theta_2)+\omega)}{4\cosh[E(\theta_1)/2T]\cosh[E(\theta_2)/2T]}. \quad \text{(A8)}$$

The low-temperature asymptotic forms of $(T_1^{-1})_{\rm stag}$ [Eqs. (4.36) and (4.37)] are obtained as follows. The $\omega$ integral in Eq. (4.35) or Eq. (A8) is cut by the temperature $\pm T$, since by performing the summation with respect to $\epsilon$ ($=\pm$) in Eq. (4.35) or Eq. (A8) one obtains (for $|\omega|\gg T$)

$$\sum_{\epsilon=\pm}\cosh\left(i\epsilon\frac{\pi}{2}\eta+\frac{\omega}{2T}\right)B\left(\frac{\eta}{2}-i\epsilon\frac{\omega}{2\pi T},1-\eta\right) \approx \sin(\pi\eta)\Gamma(1-\eta)\left(\frac{|\omega|}{2\pi T}\right)^{\eta-1}\exp\left(-\frac{|\omega|}{2T}\right). \quad \text{(A9)}$$

This can easily be verified by using the asymptotic form of the beta function:

$$B\left(\frac{\eta}{2}-iS,1-\eta\right)\approx\Gamma(1-\eta)(-iS)^{\eta-1} \quad (\text{for } S\to\pm\infty). \quad \text{(A10)}$$

Thus we have for $m_t>0$

$$(T_1^{-1})_{\rm stag} \propto T^{\eta}\int_{-\infty}^{\infty}d\theta_1 d\theta_2 d\theta_3\coth^2\left(\frac{\theta_1-\theta_2}{2}\right) \times\delta(E(\theta_1)-E(\theta_2)+E(\theta_3)) \times e^{-[E(\theta_1)+E(\theta_2)+E(\theta_3)]/2T} \propto T^{1+\eta}\exp(-2m_t/T), \quad \text{(A11)}$$

which reproduces Eq. (4.36). For $m_t<0$ we have

$$(T_1^{-1})_{\rm stag} \propto T^{\eta}\int_{-\infty}^{\infty}d\theta_1 d\theta_2\delta(E(\theta_1)-E(\theta_2)) \times e^{-[E(\theta_1)+E(\theta_2)]/2T} \propto T^{\eta}\exp(-|m_t|/T)\ln T, \quad \text{(A12)}$$

which reproduces Eq. (4.37).


[1] M. Uehara, T. Nagata, J. Akimitsu, H. Takahashi, N. Môri, and K. Kinoshita, J. Phys. Soc. Jpn. **65**, 2764 (1996); T. Nagata, M. Uehara, J. Goto, N. Komiya, J. Akimitsu, N. Motoyama, H. Eisaki, S. Uchida, H. Takahashi, T. Nakanishi, and N. Môri, Physica C **282-287**, 153 (1997).

[2] E. Dagotto and T. M. Rice, Science **271**, 618 (1996).

[3] E. Dagotto, Rep. Prog. Phys. **62**, 1525 (1999), and references therein.

[4] M. Azuma, Z. Hiroi, M. Takano, K. Ishida, and Y. Kitaoka, Phys. Rev. Lett. **73**, 3463 (1994).

[5] K. Ishida, Y. Kitaoka, K. Asayama, M. Azuma, Z. Hiroi, and M. Takano, J. Phys. Soc. Jpn. **63**, 3222 (1994).

[6] K. Kojima, A. Keren, G. M. Luke, B. Nachumi, W. D. Wu, Y. J. Uemura, M. Azuma, and M. Takano, Phys. Rev. Lett. **74**, 2812 (1995).

[7] T. Imai, K. R. Thurber, K. M. Shen, A. W. Hunt, and F. C. Chou, Phys. Rev. Lett. **81**, 220 (1998).

[8] M. Takigawa, N. Motoyama, H. Eisaki, and S. Uchida, Phys. Rev. B **57**, 1124 (1998).

[9] T. Osafune, N. Motoyama, H. Eisaki, and S. Uchida, Phys. Rev. Lett. **78**, 1980 (1997).

[10] H. Mayaffre, P. Auban-Senzier, M. Nardone, D. Jérome, D. Poilblanc, C. Bourbonnais, U. Ammerahl, G. Dhalenne, and A. Revcolevschi, Science **279**, 345 (1998).

[11] Y. Piskunov, D. Jérome, P. Auban-Senzier, P. Wzietek, C. Bourbonnais, U. Ammerhal, G. Dhalenne, and A. Revcolevschi, Eur. Phys. J. B **24**, 443 (2001).

[12] N. Fujiwara, N. Môri, Y. Uwatoko, T. Matsumoto, N. Motoyama, and S. Uchida, Phys. Rev. Lett. **90**, 137001 (2003).

[13] H. Kitano, R. Inoue, T. Hanaguri, A. Maeda, N. Motoyama, M. Takaba, K. Kojima, H. Eisaki, and S. Uchida, Europhys. Lett. **56**, 434 (2001).

[14] G. Blumberg, P. Littlewood, A. Gozar, B. S. Dennis, N. Motoyama, H. Eisaki, and S. Uchida, Science **297**, 584 (2002).

[15] B. Gorshunov, P. Haas, T. Rõõm, M. Dressel, T. Vuletić, B. Korin-Hamzic, S. Tomic, J. Akimitsu, and T. Nagata, Phys. Rev. B **66**, 060508(R) (2002).

[16] N. Motoyama, H. Eisaki, S. Uchida, N. Takeshita, N. Môri, T. Nakanishi, and H. Takahashi, Europhys. Lett. **58**, 758 (2002).

[17] T. Vuletić, B. Korin-Hamzić, S. Tomic, B. Gorshunov, P. Haas, T.

Rõõm, M. Dressel, J. Akimitsu, T. Sasaki, and T. Nagata, Phys. Rev. Lett. **90**, 257002 (2003).
[18] A. Gozar, G. Blumberg, P. B. Littlewood, B. S. Dennis, N. Motoyama, H. Eisaki, and S. Uchida, Phys. Rev. Lett. **91**, 087401 (2003).
[19] E. Dagotto, J. Riera, and D. Scalapino, Phys. Rev. B **45**, R5744 (1992).
[20] A. M. Finkel'stein and A. I. Larkin, Phys. Rev. B **47**, 10461 (1993).
[21] T. M. Rice, S. Gopalan, and M. Sigrist, Europhys. Lett. **23**, 445 (1993); S. Gopalan, T. M. Rice, and M. Sigrist, Phys. Rev. B **49**, 8901 (1994).
[22] M. Fabrizio, Phys. Rev. B **48**, 15838 (1993).
[23] M. Sigrist, T. M. Rice, and F. C. Zhang, Phys. Rev. B **49**, 12058 (1994).
[24] H. Tsunetsugu, M. Troyer, and T. M. Rice, Phys. Rev. B **49**, R16078 (1994); M. Troyer, H. Tsunetsugu, and T. M. Rice, *ibid.* **53**, 251 (1996).
[25] D. V. Khveshchenko and T. M. Rice, Phys. Rev. B **50**, 252 (1994); D. V. Khveshchenko, *ibid.* **50**, 380 (1994).
[26] R. M. Noack, S. R. White, and D. J. Scalapino, Phys. Rev. Lett. **73**, 882 (1994); Physica C **270**, 281 (1996).
[27] N. Nagaosa, Solid State Commun. **94**, 495 (1995).
[28] H. J. Schulz, Phys. Rev. B **53**, R2959 (1996); in *Correlated Fermions and Transport in Mesoscopic Systems*, edited by T. Martin, G. Montambaux, and T. Trân Thanh Vân (Editions Frontières, Gif-sur-Yvette, France, 1996), p. 81.
[29] L. Balents and M. P. A. Fisher, Phys. Rev. B **53**, 12133 (1996).
[30] E. Orignac and T. Giamarchi, Phys. Rev. B **56**, 7167 (1997).
[31] C. Wu, W. V. Liu, and E. Fradkin, Phys. Rev. B **68**, 115104 (2003).
[32] M. Vojta, R. E. Hetzel, and R. M. Noack, Phys. Rev. B **60**, R8417 (1999).
[33] M. Tsuchiizu and A. Furusaki, Phys. Rev. B **66**, 245106 (2002).
[34] E. Orignac and R. Citro, Eur. Phys. J. B **33**, 419 (2003).
[35] V. J. Emery, in *Highly Conducting One-Dimensional Solids*, edited by J. Devreese, R. Evrard, and V. van Doren (Plenum, New York, 1979), p. 247.
[36] J. Sólyom, Adv. Phys. **28**, 201 (1979).
[37] A. O. Gogolin, A. A. Nersesyan, and A. M. Tsvelik, *Bosonization and Strongly Correlated Systems* (Cambridge University Press, Cambridge, U.K., 1998).
[38] The slight difference between Eq. (2.20) and Eq. (4.27) in Ref. 33 arises from the definitions of $g_{\rho\pm}$ and $g_{\sigma\pm}$ [Eq. (2.18)].
[39] D. G. Shelton, A. A. Nersesyan, and A. M. Tsvelik, Phys. Rev. B **53**, 8521 (1996); D. G. Shelton and A. M. Tsvelik, *ibid.* **53**, 14036 (1996); A. A. Nersesyan and A. M. Tsvelik, Phys. Rev. Lett. **78**, 3939 (1997).
[40] V. J. Emery, S. A. Kivelson, and O. Zachar, Phys. Rev. B **59**, 15641 (1999).
[41] L. S. Levitov and A. M. Tsvelik, Phys. Rev. Lett. **90**, 016401 (2003); A. A. Nersesyan and A. M. Tsvelik, Phys. Rev. B **68**, 235419 (2003).
[42] S. Sachdev, *Quantum Phase Transition* (Cambridge University Press, Cambridge, U.K., 1999).
[43] P. D. Francesco, P. Mathieu, and D. Sénéchal, *Conformal Field Theory* (Springer-Verlag, New York, 1997).
[44] U. Ledermann, K. Le Hur, and T. M. Rice, Phys. Rev. B **62**, 16383 (2000).
[45] M. Tsuchiizu, P. Donohue, Y. Suzumura, and T. Giamarchi, Eur. Phys. J. B **19**, 185 (2001); P. Donohue, M. Tsuchiizu, T. Giamarchi, and Y. Suzumura, Phys. Rev. B **63**, 045121 (2001).
[46] H. J. Schulz, Phys. Rev. B **59**, R2471 (1999).
[47] R. Konik, F. Lesage, A. W. W. Ludwig, and H. Saleur, Phys. Rev. B **61**, 4983 (2000).
[48] T. Siller, M. Troyer, T. M. Rice, and S. R. White, Phys. Rev. B **63**, 195106 (2001).
[49] M. Tsuchiizu and Y. Suzumura, J. Phys. Soc. Jpn. **73**, 804 (2004).
[50] A. M. Tsvelik, Phys. Rev. B **42**, 10499 (1990).
[51] O. A. Starykh and L. Balents, Phys. Rev. Lett. **93**, 127202 (2004).
[52] P. Azaria, P. Lecheminant, and A. M. Tsvelik, cond-mat/9806099 (unpublished).
[53] P. Azaria, A. O. Gogolin, P. Lecheminant, and A. A. Nersesyan, Phys. Rev. Lett. **83**, 624 (1999).
[54] R. Assaraf, P. Azaria, E. Boulat, M. Caffarel, and P. Lecheminant, Phys. Rev. Lett. **93**, 016407 (2004).
[55] C. Bourbonnais and L. G. Caron, Int. J. Mod. Phys. B **5**, 1033 (1991); C. Bourbonnais, J. Phys. I **3**, 143 (1993).
[56] H. Nélisse, C. Bourbonnais, H. Touchette, Y. M. Vilk, and A.-M. S. Tremblay, Eur. Phys. J. B **12**, 351 (1999).
[57] J. Kishine and H. Fukuyama, J. Phys. Soc. Jpn. **66**, 26 (1997); J. Kishine, *ibid.* **66**, 1229 (1997).
[58] D. A. Ivanov and P. A. Lee, Phys. Rev. B **59**, 4803 (1999).
[59] K. Damle and S. Sachdev, Phys. Rev. B **57**, 8307 (1998).
[60] R. Citro and E. Orignac, Phys. Rev. B **65**, 134413 (2002).
[61] M. Tsuchiizu, H. Yoshioka, and Y. Suzumura, Prog. Theor. Phys. **98**, 1045 (1997).
[62] M. Troyer, H. Tsunetsugu, and D. Würtz, Phys. Rev. B **50**, 13515 (1994).
[63] T. Moriya, J. Phys. Soc. Jpn. **18**, 516 (1963).
[64] A. W. Sandvik, E. Dagotto, and D. J. Scalapino, Phys. Rev. B **53**, R2934 (1996).
[65] F. Naef and X. Wang, Phys. Rev. Lett. **84**, 1320 (2000).
[66] J. Sagi and I. Affleck, Phys. Rev. B **53**, 9188 (1996).
[67] H. J. Schulz, Phys. Rev. B **34**, 6372 (1986).
[68] S. Sachdev, T. Senthil, and R. Shankar, Phys. Rev. B **50**, 258 (1994).
[69] S. Eggert, I. Affleck, and M. Takahashi, Phys. Rev. Lett. **73**, 332 (1994).
[70] H. M. Babujian, Nucl. Phys. B **215**, 317 (1983).
[71] V. Barzykin, Phys. Rev. B **63**, 140412(R) (2001)
[72] A. LeClair, F. Lesage, S. Sachdev, and H. Saleur, Nucl. Phys. B **482**, 579 (1996).